geodiversitas

2022 • 44 • 15

# The Vallesian large *Palaeotragus* Gaudry, 1861 (Mammalia: Giraffidae) from Northern Greece

Kostantis LASKOS & Dimitris S. KOSTOPOULOS

art. 44 (15) — Published on 14 April 2022
www.geodiversitas.com

PUBLICATIONS SCIENTIFIQUES

MUSÉUM NAL HIST NATURELLE

*Geodiversitas* est indexé dans / Geodiversitas *is indexed in:*
– Science Citation Index Expanded (SciSearch®)
– ISI Alerting Services®
– Current Contents® / Physical, Chemical, and Earth Sciences®
– Scopus®

*Geodiversitas* est distribué en version électronique par / Geodiversitas *is distributed electronically by:*
– BioOne® (http://www.bioone.org)

Les articles ainsi que les nouveautés nomenclaturales publiés dans *Geodiversitas* sont référencés par / *Articles and nomenclatural novelties published in* Geodiversitas *are referenced by:*
– ZooBank® (http://zoobank.org)

***Geodiversitas*** est une revue en flux continu publiée par les Publications scientifiques du Muséum, Paris
**Geodiversitas** *is a fast track journal published by the Museum Science Press, Paris*

Les Publications scientifiques du Muséum publient aussi / *The Museum Science Press also publish:* ***Adansonia***, ***Zoosystema***, ***Anthropozoologica***, ***European Journal of Taxonomy***, ***Naturae***, ***Cryptogamie*** **sous-sections** ***Algologie***, ***Bryologie***, ***Mycologie, Comptes Rendus Palevol***

Diffusion – Publications scientifiques Muséum national d'Histoire naturelle
CP 41 – 57 rue Cuvier F-75231 Paris cedex 05 (France)
Tél. : 33 (0)1 40 79 48 05 / Fax : 33 (0)1 40 79 38 40
diff.pub@mnhn.fr / http://sciencepress.mnhn.fr


ISSN (imprimé / *print*) : 1280-9659/ ISSN (électronique / *electronic*) : 1638-9395

# The Vallesian large *Palaeotragus* Gaudry, 1861 (Mammalia: Giraffidae) from Northern Greece

**Kostantis LASKOS**
**Dimitris S. KOSTOPOULOS**
Laboratory of Palaeontology, School of Geology,
Aristotle University of Thessaloniki, 54124 Thessaloniki (Greece)
konslask@gmail.com
dkostop@geo.auth.gr (corresponding author)

Submitted on 10 November 2020 | accepted on 6 January 2021 | published on 14 April 2022

urn:lsid:zoobank.org:pub:95BA3F3F-02AB-467E-AF22-4113AD4F492A

Laskos K. & Kostopoulos D. S. — The Vallesian large *Palaeotragus* Gaudry, 1861 (Mammalia: Giraffidae) from Northern Greece. *Geodiversitas* 44 (15): 437-470. https://doi.org/10.5252/geodiversitas2022v44a15. http://geodiversitas.com/44/15

**ABSTRACT**
We herein re-discuss the systematics of the Late Miocene representatives of the most common but poorly documented Eurasian giraffid genus *Palaeotragus* on the occasion of the review and description of new samples from the Vallesian faunas of Northern Greece. Our results detect five Late Miocene *Palaeotragus* morphotypes, recognizing at least four species. The so called 'small-sized palaeotrages' are represented by the type species *P. rouenii* and the Chinese *P. microdon*, whereas the validity of *P. pavlowae* from Grebeniki (Ukraine) is doubted. 'Large-sized palaeotrages' are mainly represented by *P. coelophrys* (synonym of *P. expectans, P. borissiaki, P. hoffstetteri, P. quadricornis,* and probably *P. moldavicus*), a species that thrived in the peri- Black Sea territories during Vallesian and survived during Turolian in the Irano-Anatolian domain, likely by adopting a more robust appearance. Large palaeotrages from the Vallesian faunas of Pentalophos and Ravin de la Pluie (Axios Valley, Greece) are identified as *P. coelophrys* with certain confidence. The Vallesian *P. berislavicus* from Berislav (Ukraine) has intermediate morphometric features between *P. rouenii* and *P. coelophrys* and it is, therefore, recognized as a most probably valid species. The latest Vallesian Nikiti-1 (Chalkidiki peninsula) large palaeotrage shares many morphometric features with *P. berislavicus*, suggesting that the species may have invaded Balkans by the end of Vallesian and possibly survived there until middle Turolian. The Late Miocene *Palaeotragus asiaticus* from Central Asia is a quite problematic species; it appears closely related to the Turolian equivalent *P.* cf. *coelophrys* from China and both may be linked to the older Berislav taxon.

**KEY WORDS**
Late Miocene,
Palaeotragiinae,
giraffes,
Europe.

**RÉSUMÉ**
*Les* Palaeotragus *Gaudry, 1861 (Mammalia: Giraffidae) du Vallésien de Grèce du Nord.*
Nous re-discutons ici de la systématique des représentants du Miocène supérieur du genre de girafide eurasien le plus commun mais mal documenté, *Palaeotragus* à l'occasion de revision et de la description originale de matériel vallésiens du nord de la Grèce. Nos résultats permettent de détecter cinq morphotypes de *Palaeotragus* du Miocène supérieur, reconnaissant au moins quatre espèces. Les « paléotrages de petite taille» sont représentés par l'espèce type *P. rouenii* et *P. microdon* chinoise, alors que la validité de *P. pavlowae* de Grebeniki, Ukraine est mise en doute. Les « paléotrages de grande taille » sont principalement représentés par *P. coelophrys* (synonyme de *P. expectans, P. borissiaki, P. hoffstetteri, P. quadricornis*, et probablement *P. moldavicus*), une espèce qui a prospéré dans les territoires péri-Mer Noire pendant Vallesian et a survécu au Turolien dans le domaine irano-anatolien, probablement en adoptant une apparence plus robuste. De grands paléotrages des faunes vallésiennes du Pentalophos et du Ravin de la Pluie (vallée d'Axios, Grèce) sont attribués à *P. coelophrys* avec une certaine confiance. Le vallésien paléotrage de Berislav (*P. berislavicus*) d'Ukraine présente des caractéristiques morphométriques intermédiaires entre *P. rouenii* et *P. coelophrys* et il est donc reconnu comme une espèce très probablement valide. Le grand paléotrage de Nikiti-1 (péninsule de Chalcidique) présente des ressemblances importantes avec *P. berislavicus*, ce qui suggère que l'espèce pourrait envahir les Balkans à la fin du Vallésien et y survivre jusqu'au Turolien moyen. *Palaeotragus asiaticus* d'Asie centrale est une espèce assez problématique; il apparaît étroitement lié à *P.* cf. *coelophrys* de Chine et les deux peuvent être liés à l'ancien taxon de Berislav.

**MOTS CLÉS**
Miocène supérieur,
Palaeotragiinae,
girafes,
Europe.

## INTRODUCTION

Palaeotragiinae is probably a polyphyletic or paraphyletic subfamily including species of the genus *Palaeotragus*, and according to some authors members of *Samotherium* too (Geraads 1986; Godina 2002; Hou *et al.* 2014; Danowitz *et al.* 2015). A phylogenetic parsimony analysis by Ríos *et al.* (2017: 31) restricted on the most well-known species supports, however, the genus monophyly. *Palaeotragus* was the most common giraffid genus of Eurasia during the Late Miocene, expanded from North Africa to the Black Sea and from the Balkans to China. It achieved maximal dispersion and diversity in the Turolian mammal communities of Eastern Mediterranean.

Numerous species have been ascribed to *Palaeotragus* from the Miocene of the Old World, most of them from the Late Miocene of W. Eurasia. The type species is *Palaeotragus rouenii* Gaudry, 1861, originally from Pikermi (Greece), archetype of the so-called 'small-sized palaeotrages'. Another widely accepted taxon is *Palaeotragus coelophrys* (Rodler & Weithofer, 1890) originally from Maragheh (Iran), usually regarded as the basic model of a 'large-sized palaeotrage'. Other Eurasian Late Miocene palaeotragine taxa include: *Palaeotragus microdon* (Koken, 1885) from Shansi (China); *Palaeotragus asiaticus* Godina, 1975 from Ortok (Kyrgyzstan); *Palaeotragus borissiaki* (Alexeev, 1930) from Eldari (Georgia); *Palaeotragus expectans* (Borissiak, 1914) from Sevastopol, *Palaeotragus pavlowae* (Pavlow, 1913) from Grebeniki, *Palaeotragus berislavicus* Korotkevitch, 1957 from Berislav (Ukraine); *Palaeotragus moldavicus* Godina, 1979 from Starye Bogeny (Moldova); *Palaeotragus hoffstetteri* Ozansoy, 1965 from Sinap (Turkey); and *Palaeotragus quadricornis* Bohlin, 1926 from Samos (Greece). The validity, generic affiliations and supra-generic relationships of most of these species are, however, strongly debated (e.g., Geraads 1974, 1986; Godina 1975, 1979; Ríos *et al.* 2017).

In Greece, *Palaeotragus* oldest record is from the Vallesian faunas of Axios Valley (Koufos 2006), whereas its last occurrence is from the Early Pleistocene faunas of continental Greece and Lesvos Island (Steensma 1988; Kostopoulos & Koufos 1994; de Vos *et al.* 2002; Athanassiou 2014). During the Turolian, the genus was mainly represented in the local mammal assemblages by the small and slender *P. rouenii* (Iliopoulos 2003; Koufos 2006; Kostopoulos 2009; Koufos *et al.* 2016; Lazaridis 2015; Xafis *et al.* 2019). Late Miocene large sized palaeotrages are rather scarce in the Greek record (Fig. 1), including sparse findings from the Vallesian faunas of Pentalophos, Xirochori, Ravin de la Pluie (Axios valley) and Nikiti-1 (Chalkidiki peninsula), as well as from the Turolian faunas of Kerassia, Samos and Thermopigi (Geraads 1979; Iliopoulos 2003; Kostopoulos 2009; Xafis *et al.* 2019).

The main aim of this study is the taxonomic review of the Vallesian large sized *Palaeotragus* from Northern Greece. The studied material comes from the Upper Miocene fossil sites of Nikiti-1 (NKT) in the Chalkidiki peninsula, and Pentalophos (PNT), Ravin de la Pluie (RPl) and Xirochori (XIR) at the Axios Valley (Fig. 1). The geological, stratigraphic and chronological settings of both fossiliferous areas are provided by Koufos (1990, 2016), Koufos *et al.* (1991), and Sen *et al.* (2000). The PNT material was previously referred to *Palaeotragus coelophrys* (Koufos 2006; Konidaris 2013) but never described; the associated fauna is suggested as of early late Vallesian, (latest MN9; Koufos 2006; Konidaris

2013). The large-sized *Palaeotragus* material from RPl was attributed to *Palaeotragus* cf. *coelophrys* by Geraads (1978), whereas the poor XIR material remained unpublished until now; faunal assemblages of both RPl and XIR are suggested as late Vallesian (MN10; Koufos 2006; Konidaris 2013). The NKT material was originally described as *Palaeotragus* cf. *rouenii* (Kostopoulos *et al.* 1996) and later considered as *Palaeotragus* sp. (Koufos *et al.* 2016); the NKT fauna is suggested as of latest Vallesian age (latest MN10; Koufos *et al.* 2016). The revision of the Greek Vallesian large-sized *Palaeotragus* leads to the necessary reassessment of the systematics of Late Miocene Eurasian large sized *Palaeotragus*.

## MATERIAL AND METHODS

We follow the nomenclature proposed by Gentry *et al.* (1999) for the adult dental material; Geraads *et al.* (2013) for the deciduous lower premolars; Ríos *et al.* (2016) for the metapodials; Solounias & Danowitz (2016) for the astragali; and Schmid (1972) for the other postcranials. Postcranial measurements are according to the system proposed by von der Driesch (1976).

In order to test possible groupings within Late Miocene *Palaeotragus* species we performed Principal Coordinates Analysis (PCO) with Gower similarity, and Principal Components Analysis (PCA) based on 12 dental metrical features and indices, 15 postcranial measures and indices and 4 qualitative characters of $P_3$ and $P^4$ morphology (see Appendix 1). As available material appears fragmentary in several cases, the original dataset suffers from a rather high number of missing values. They are treated by iterative imputation option in PCA, whereas a series of subsequent analyses of both PCA and PCO were run by omitting taxa and/or parameters to test consistency of the results. A set of scatter diagrams based on selected and better documented variables associates multivariate analyses.

The PAST software (Hammer *et al.* 2001) was used for the statistical analyses. The program Inkscape was used for the illustrations provided. The program Adobe Photoshop was used for the processing of the studied material from NKT, PNT and RPl. All studied material is housed in the Museum of Geology-Palaeontology-Palaeoanthropology of the Aristotle University of Thessaloniki (LGPUT).

### Abbreviations

| | |
|---|---|
| AMNH | American Museum of Natural History, New York; |
| LGPUT | Museum of Geology – Palaeontology – Palaeoanthropology, Aristotle University of Thessaloniki; |
| NHM | Natural History Museum, Izmir; |
| MNHN | Muséum national d'Histoire naturelle, Paris; |
| OSU | Odessa State University, Odessa; |
| PIN | Palaeontological Institute, Moscow; |
| RSGU | Russian State Geological Prospecting University, Moscow; |
| SIZK | Schmalhausen Institute of Zoology of National Academy of Sciences of Ukraine, Kyiv; |
| SIT | Thermopigi Local Palaeontological Collection, Serres Prefecture, Greece. |

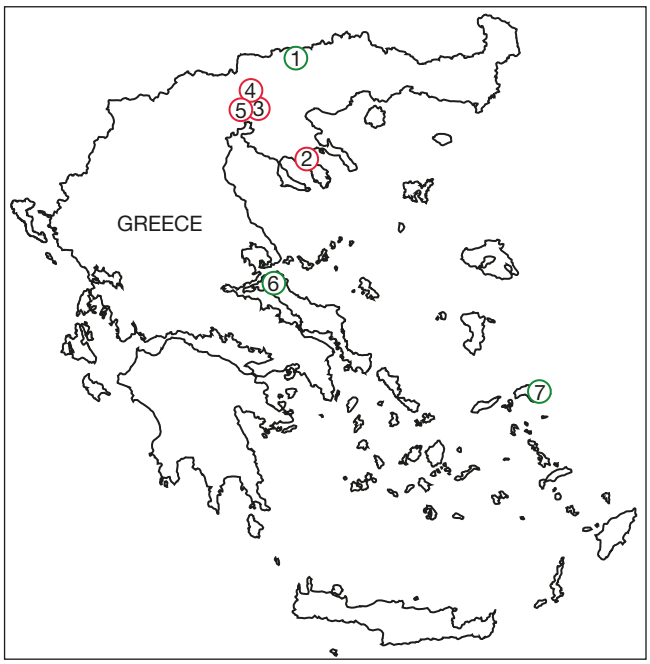


Fig. 1. — Occurrences of large sized *Palaeotragus* Gaudry, 1861 in Greece: **1**, Thermopigi; **2**, Nikiti-1; **3**, Pentalophos; **4**, Xirochori; **5**, Ravin de la Pluie; **6**, Kerassia; **7**, Mytilinii, Samos. **Red circles**, Vallesian occurrences; **green circles**, Turolian occurrences.

## SYSTEMATIC PALAEONTOLOGY

Order ARTIODACTYLA, Owen 1848
Family Giraffidae Gray, 1821
Subfamily Palaeotragiinae Pilgrim, 1911

Genus *Palaeotragus* Gaudry, 1861

Type species. — *Palaeotragus rouenii* Gaudry, 1861 by original designation.

Type locality. — Pikermi, Greece.

Age. — Late Miocene to Early Pleistocene.

Generic diagnosis (based on Geraads 1974; Churcher 1978). — Giraffids of small to medium size. Skull wide with long postorbital cranial part. Ossicones simple, straight to slightly curved with smooth surface, single paired, pointed, uprightly inserted on frontals in supraorbital position, widely spaced on the cranial roof, and subparallel to each other. Frontals concave between the ossicones. Diastema long; dentition brachydont, premolar section proportionally long. Metapodials elongate, slender with moderately to strongly deep central palmar/plantar through.

### Description

*Pentalophos sample (end MN9)*

**Studied material (LGPUT, *Palaeotragus coelophrys*).** Right maxilla with $P^2$-$M^3$ (PNT-113); part of left maxilla with $M^2$-$M^3$ (PNT-165); upper right $P^2$ (PNT-161); upper right $P^2$-$P^3$ (PNT-162); upper right $P^2$-$P^3$ (PNT-163); upper left $P^3$ (PNT-164); part of right mandible with $M_1$-$M_3$ (PNT-328F); part of right mandible

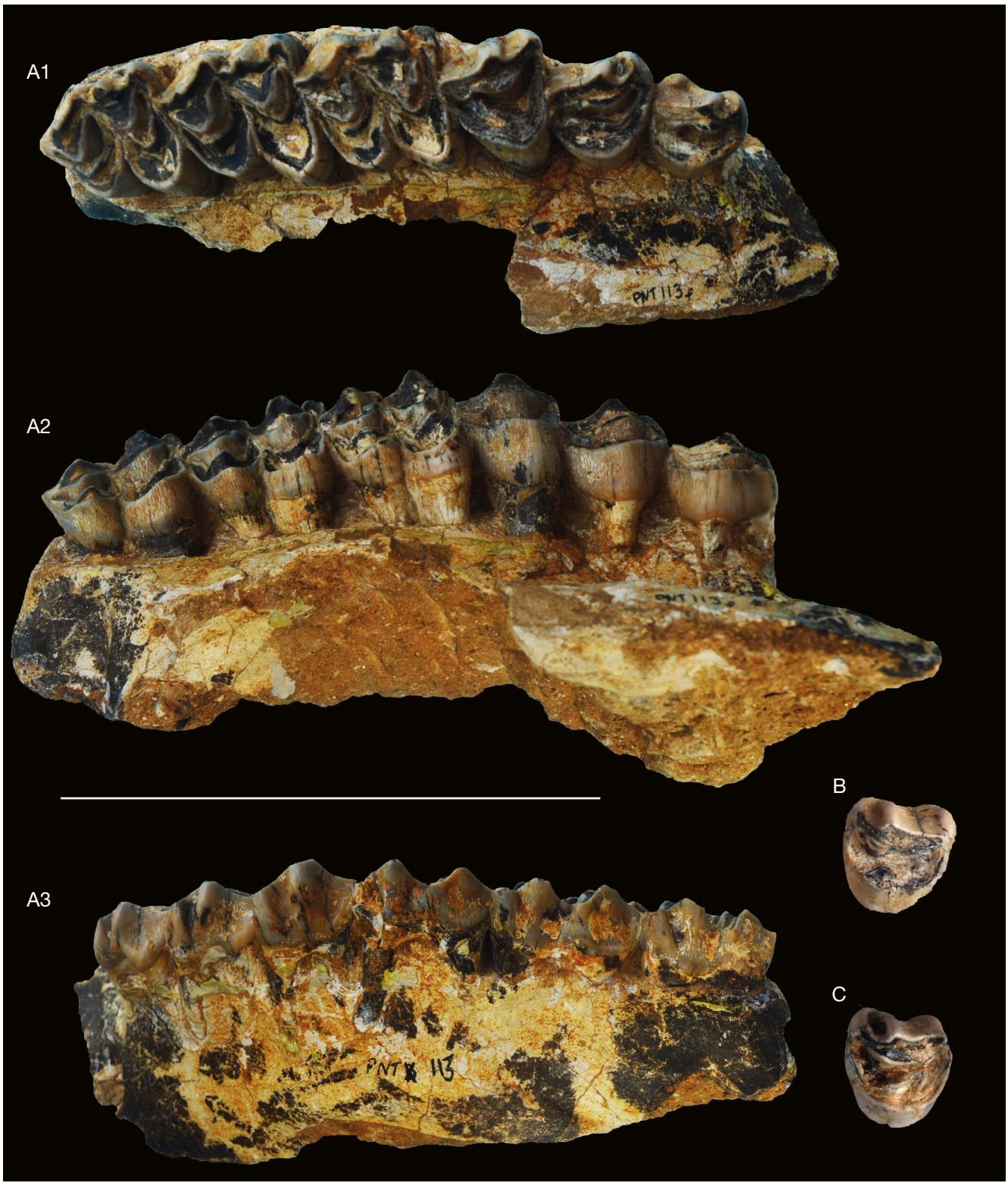


Fig. 2. — *Palaeotragus coelophrys* (Rodler & Weithofer, 1890) from Pentalophos, Axios Valley, Greece (late early Vallesian): **A**, upper toothrow LGPUT PNT-113F: **1**, occlusal; **2**, lingual; **3**, labial views; **B**, upper $P^2$ (LGPUT PNT-161) in occlusal view; **C**, upper $P^3$ (LGPUT PNT-164) in occlusal view. Scale bar: 10 cm.

with $dP_2$-$M_1$ (PNT-121F); distal part of left humerus (PNT-166); proximal parts of a right and a left metatarsal (PNT-114F, PNT-119F). The taxon is represented by at least four adult and a juvenile individual. Measurements are provided in Appendix 2: Tables 1-4.

**Upper dentition**. All the labial ribs and styles of the premolars (parastyle, paracone, metastyle) are well developed (Fig. 2A-C; Table 1). The hypocone is weak, but distinct. The enamel is finely rugose especially on the lingual side

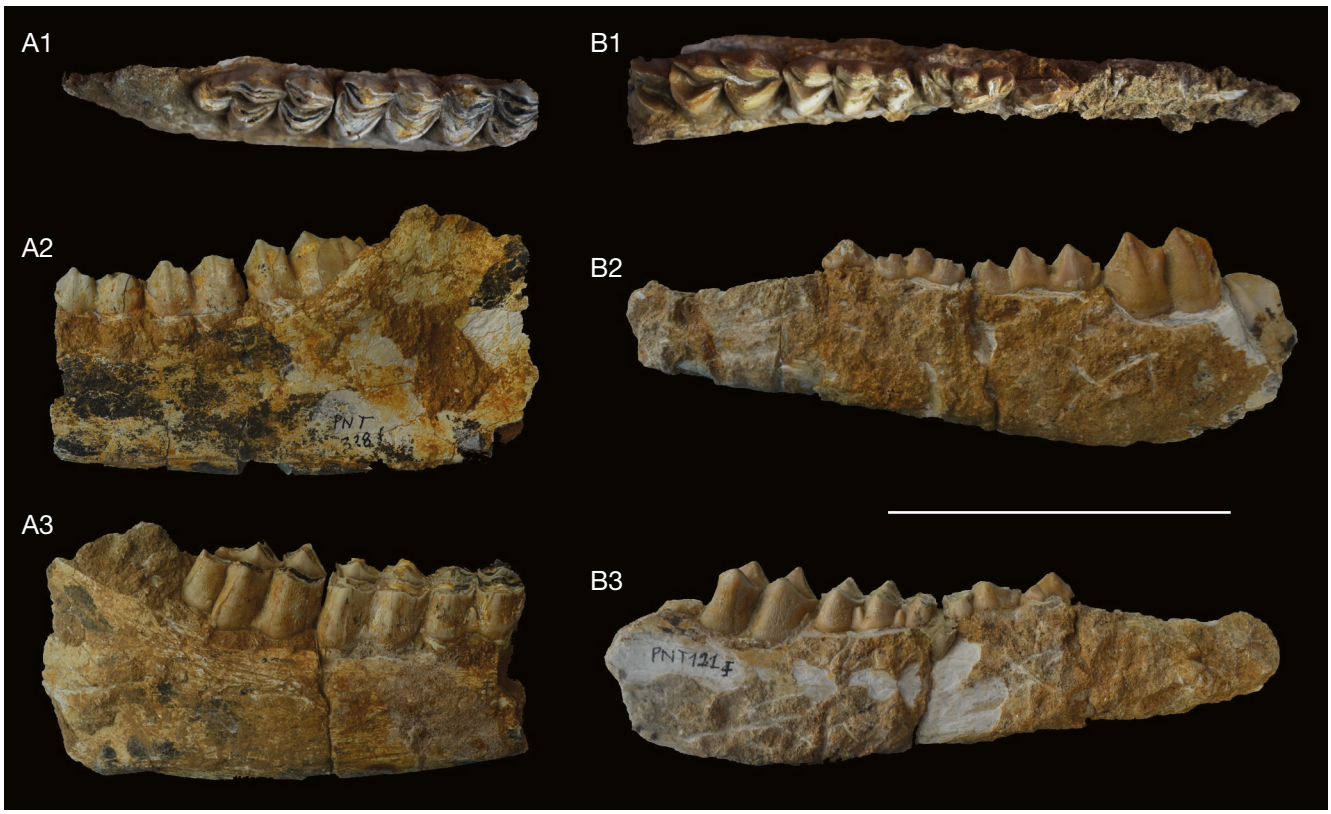


FIG. 3. — *Palaeotragus coelophrys* (Rodler & Weithofer, 1890) from Pentalophos, Axios Valley, Greece (late early Vallesian): **A**, part of mandible with $M_1$-$M_3$, LGPUT PNT-328F; **B**, part of deciduous mandible with $dP_2$-$M_1$, LGPUT PNT-121F; **1**, occlusal; **2**, lingual; **3**, labial views. Scale bar: 10 cm.

of the premolars. In some of the premolars there is a well-developed lingual cingulum (PNT-161, PNT-164; Fig. 2B, C). In the preserved $P^2$ and $P^3$ (Fig. 2A-C) the parastyle and the paracone rib are close to each other and the enamel is folded in the area of the parastyle towards the paracone. Moreover, these teeth are inflated at the basis, lingually rounded and they delineate occlusally an almost half circle. The $P^2$ of the PNT-113 toothrow (Fig. 2A) has a prominent disto-labial style that reaches almost ⅓ of the crown's height. In the single available $P^4$, the paracone is more centrally placed, still slightly folded towards the parastyle, and the tooth has a triangular occlusal shape. The fossettes of the $P^2$ are distorted, but they look wide. The fossettes of the $P^3$ and $P^4$ are also wide and bear a hypoconal fold distally.

The upper molars are similar to those of other giraffids (Fig. 2A). The most prominent labial features are the parastyle, the paracone rib and the mesostyle. The metastyle is barely developed in the $M^1$-$M^2$, but similarly strong to the parastyle in the $M^3$. Lingually, the protocone is more prominent than the hypocone, especially in the $M^3$; hence the mesial lobe is wider and square shaped whereas the distal lobe is narrower and rounder. The fossettes converge towards the center of the tooth but they do not fuse. The hypocone flange reaches almost at the labial side of the molar, stopping just before the mesostyle mesially and the metastyle distally. The protocone flange almost reaches the parastyle mesially. Distally, it reaches almost at the center of the tooth. The enamel is finely rugose in all the molars, which also have a fine cement cover, mainly labially. Although in a less advanced wear stage, PNT-165 upper molars share the same basic morphological features with those of PNT-113. A lingual cingulum, occurs, especially on the mesial lobe.

**Lower dentition**. The right mandible PNT-328F preserves only the molars (Fig. 3A; Table 2). The mandibular height is 48.9 mm at the $M_1$-$M_2$ level, and 53.6 mm below the distal lobe of $M_3$. All the lower molars preserve a fine cement cover. The most prominent lingual feature is the metastylid, and then the metaconid; the entoconid is traceable but less strong. In the disto-lingual side of the $M_1$ and $M_2$ the entoconulid is present but not prominent. The entoconulid of the $M_2$ is completely separated from the hypocone region in the upper part of the crown. The same applies probably for the entoconulid of $M_1$. The praentocristid penetrates in the mesial fossette, separating the labial and lingual side of the mesial lobe. The protoconid and the hypoconid are almost equally developed. An ectostylid is present on $M_1$, less developed on $M_2$, and absent on $M_3$. Finally, the hypoconulid is pointed labially and parallel to the protoconid and hypoconid. Lingually, the third lobe of the $M_3$ is separated from the second one by a shallow furrow. The cingulum appears strong on $M_1$, but weak on $M_2$ and absent on $M_3$.

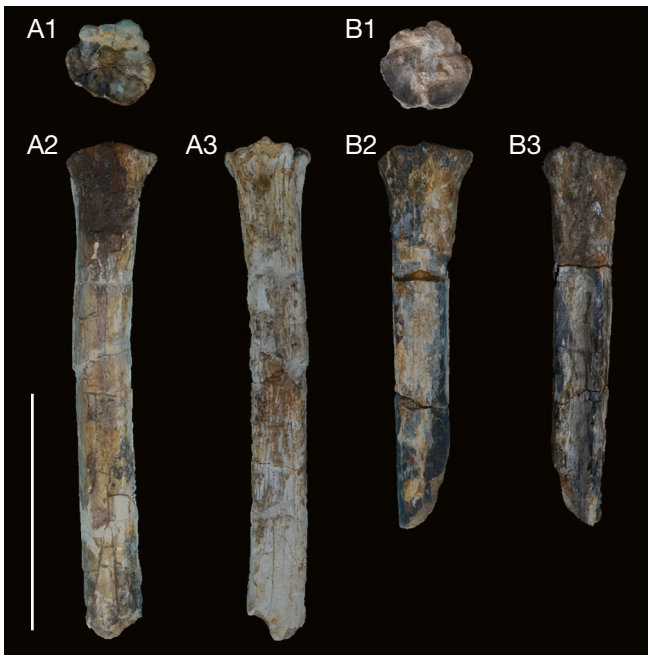


FIG. 4. — Partial metatarsals of *Palaeotragus coelophrys* (Rodler & Weithofer, 1890) from Pentalophos, Axios Valley, Greece (late early Vallesian): **A**, LGPUT PNT-114F; **B**, LGPUT PNT-119F; **1**, proximal; **2**, dorsal; **3**, plantar views. Scale bar: 15 cm.

**Lower deciduous dentition**. The right mandible PNT-121F (Fig. 3B; Table 3) consists of the series of the deciduous premolars and the $M_1$. The $dP_2$ has a primitive morphology. The paraconid and anteparaconid are barely distinguished from each other. The protoconid is placed medially and it is the more developed conid. Distally, the entoconid and the hypoconulid are distinguished in the upper part of the crown, whereas they fuse in the lower. The hypoconid is prominent, placed more labially.

On the $dP_3$ the paraconid and anteparaconid are pointed lingually and they are well-distinguished in the upper half of the crown, whereas they fuse each other towards the base. The metaconid and the protoconid are the most prominent features (especially the protoconid); they fuse distally and they are folded and oriented mesially. The mesosinusid is lingually open. The distal and mesial part of the $dP_3$ are clearly separated in the area of the metaconid and protoconid fusion. The hypoconulid is as developed as the protoconid. The hypoconulid and the entocristid are distinguished only in the upper part of the crown. The metasinusid is clear but weaker than the mesosinusid.

The $dP_4$ has two prominent ectostylids. The mesial lobe is distorted, although it seems that its ribs and stylids are weaker. In the two distal lobes the labial cones are equally developed. The lingual ribs and stylids are weaker too, as in the mesial lobe. The distal flange of the third labial cone reaches the lingual side of the tooth. The distal flange of the second labial cone is also well-developed and it is placed next to the metastylid; it is the feature that separates the second from the third lobe.

The $M_1$ morphology agrees with the morphology of the $M_1$ from the adult toothrow PNT-328F: the metaconid, metastylid, entoconid and entoconulid ribs are quite well-developed in the upper half of the crown.

**Postcranials**. The distal part of the left humerus PNT-166 is badly preserved prohibiting a detailed morphological description. The olecranon fossa is rather long, narrow, and deep. The lateral supracondyloid crest is well developed and raises quite high on the distal diaphysis. Both the radial and coronoid fossae are shallow and weakly separated by each other (but also probably due to the bad preservation). The distal trochlea is asymmetric and its keel wide and rather blunt. In lateral view, the lateral epicondyle slopes weakly downwards, whereas in medial view the medial epicondyle is perpendicular compared to the diaphysis longitudinal axis and not significantly protruding.

The preserved proximal parts of the metatarsals PNT-114F and PNT-119F (Fig. 4A, B; Table 4) indicate rather long but relatively robust metapodials. On the proximal articular surface, the plantal and dorsal heads of the medial epicondyle are separated by a bone protrusion, whereas a groove separates the two heads on the lateral side. The plantar head does not tilt medially or laterally. The lateral dorsal head is placed parallel to the proximal articular surface's axis. The pygmaios is present but rather small and not prominent.

*Ravin de la Pluie sample (MN10)*

**Studied material (LGPUT, *Palaeotragus* cf. *coelophrys*)**. A 'hornless' skull with a highly worn toothrow (RPl-91B); part of right mandible, with highly worn $M_1$-$M_3$ (RPl-104F); isolated upper molar ($M^1$ or $M^2$) (RPl-315n). The taxon is represented by at least an adult and an old individual. Dental measurements are provided in Appendix 2: Table 5.

**Cranium (RPl-91B)**. The skull is strongly deformed (Fig. 5), and hence a thorough description is prevented. Geraads (1978) provided the basic recognizable cranial and dental features; we repeat here the most important ones and add a few more. The cranium lacks ossicones, and has a flattened frontal region (Fig. 5B) suggesting a female individual. The parietal region is highly lateromedially compressed. The postorbital region is elongated. The mesial border of the orbit reaches almost at the level of the center of the $M^3$ (Fig. 5A). The length from the mesial margin of the orbit to the mesial root of $P^2$ is 153.8 mm. The height of the orbit is 58.9 mm, while its horizontal (caudo-rostral) diameter is 59.2 mm. The width of the region of the frontal bone behind the orbits is 95.4 mm.

**Upper dentition**. The toothrow of the cranium RPl-91B is strongly worn (Fig. 5C). The premolars' width is similar to that of the molars, especially the width of the $P^4$. The $P^2$ and $P^3$ are lingually rounded. Labially, the parastyle, paracone rib, and metastyle are all well-developed, with the paracone rib set mesially and close to the parastyle. The premolar fossettes demonstrate a slight hypoconal fold. $P^4$ is labially

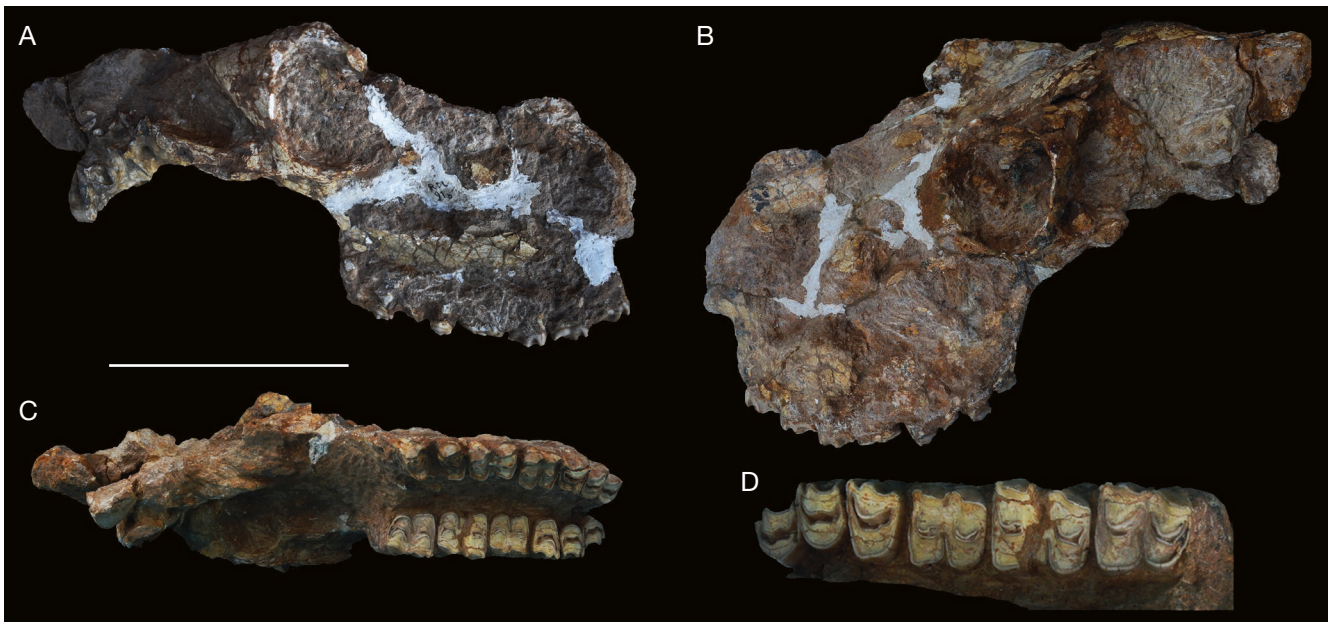


Fig. 5. — Partial cranium, LGPUT RPl 91-B of *Palaeotragus* cf. *coelophrys* from Ravin de la Pluie, Axios Valley, Greece (late Vallesian): **A**, right-lateral; **B**, left-lateral; **C**, ventral views. Scale bar: 15 cm.

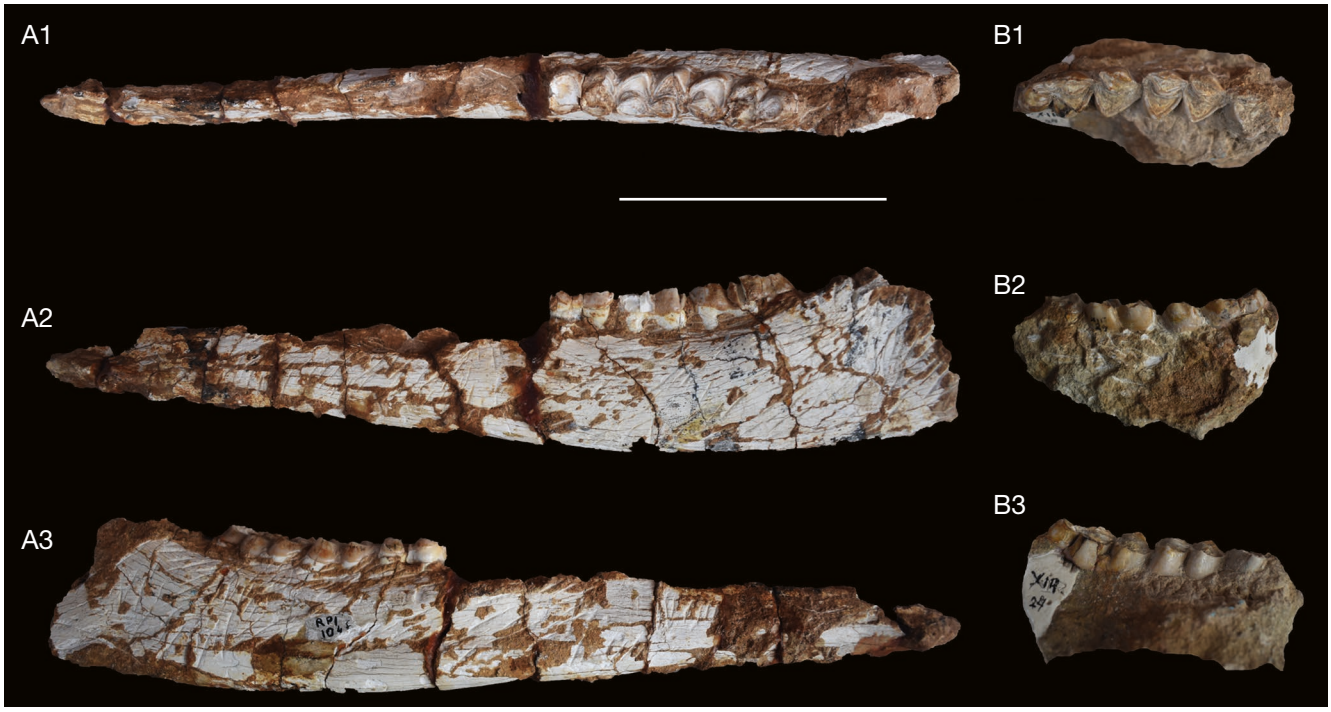


Fig. 6. — **A**, Part of mandible, LGPUT RPl-104F with $M_1$-$M_3$ of *Palaeotragus* cf. *coelophrys* from Ravin de la Pluie, Axios Valley, Greece (late Vallesian) in: **1**, occlusal; **2**, lingual; **3**, labial views; **B**, part of mandible, LGPUT XIR-24 with $M_2$-$M_3$ of *Palaeotragus* sp. from Xirochori, Axios Valley, Greece (late Vallesian) in: **1**, occlusal; **2**, lingual; **3**, labial views. Scale bar: 10 cm.

more flattened and more pointed lingually than the $P^2$ and $P^3$; a weak, shallow lingual furrow unequally divides the lingual cone. $P^4$ also has a strong parastyle, paracone rib and metastyle. The upper molars have a thin cement cover labially. The protocone widens significantly at the basal part of the crown; it is slightly constricted lingually on $M^1$ and $M^2$, and more angular on $M^3$. The labial ribs and styles are extremely worn but apart from the parastyle they do not seem well-developed.

**Lower dentition**. The mandible RPl-104F preserves only the molars (Fig. 6A; Table 6). The mandibular height is 48.9 mm at the level of $M_1$-$M_2$ and 53.6 mm at level of the distal lobe of the $M_3$. The lingual ribs seem very weak though the dentition

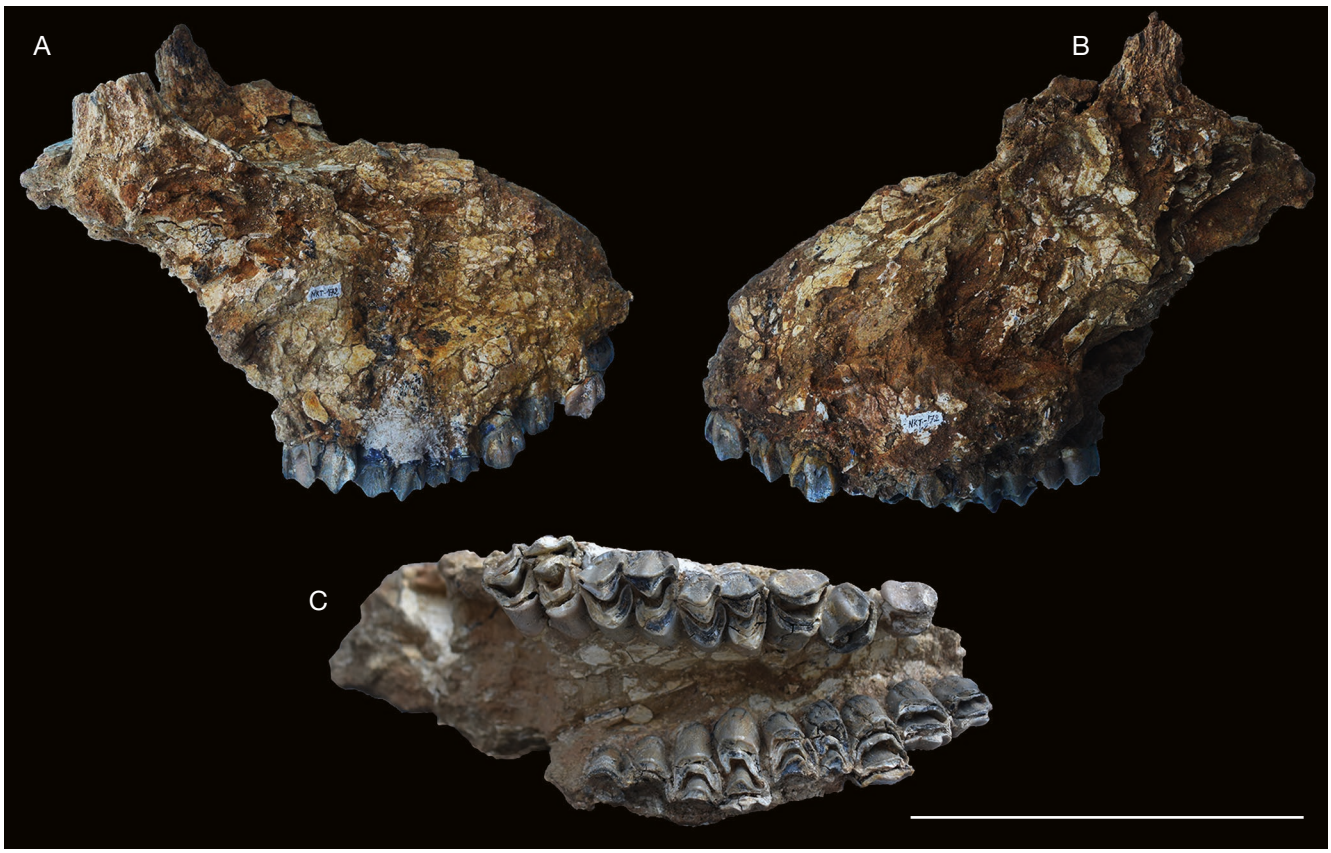


Fig. 7. — Partial cranium, LGPUT NKT-172 of *Palaeotragus* aff. *berislavicus* from Nikiti-1, Chalkidiki peninsula, Greece (latest Vallesian) in: **A**, right-lateral; **B**, left-lateral; **C**, palatal views. Scale bar: 15 cm.

is in a very advanced wear stage. Labially, the lobes of the $M_1$, and but less those of $M_2$ are pointed and centrally oriented, while those of $M_3$ are directed more distally. The distal (3rd) lobe of $M_3$ is quite large and disto-labially oriented, separated lingually from the rest of the tooth by a slight groove. There is no evidence of cingulum or cement on the molars.

*Xirochori sample (MN10)*

**Studied material (LGPUT, *Palaeotragus* sp.).** Right mandible fragment with $M_2$-$M_3$ (XIR-24). The taxon is represented by a single adult individual. Measurements are provided in Appendix 2: Table 7.

The lingual ribs and stylids are weak on the preserved $M_2$ and $M_3$ of XIR-24 (Fig. 6B) but the metaconid and the metastylid are quite prominent. The second and third lobes of the $M_3$ are separated by a very shallow groove. Labially, the protoconid and the hypoconid direct distally and they are both fairly more pointed in the $M_2$ than in the $M_3$. A weak entoconid is observed on the $M_2$. A strong ectoconid is observed between the first and the second lobe of $M_3$, while there is a weaker one between the second and the third lobe. Neither cingulum nor cement are observed.

*Nikiti-1 sample (end MN10)*

**Studied material (LGPUT, *Palaeotragus* aff. *berislavicus*).** A partial cranium preserving both toothrows and the very proximal part of the ossicones (NKT-172); a left humerus distal articulation (NKT-161); three left radii (NKT-156, NKT-159, NKT-169); a right radius (NKT-155); a proximal part of radius (NKT-167); two right metacarpals (NKT-137, NKT-141); a left metacarpal (NKT-131); two proximal parts of left metacarpals (NKT-26, NKT-67); a right tibia (NKT-271); two distal parts of tibia (NKT-150, NKT-154); two left astragali (NKT-163, NKT-266); a right astragalus (NKT-267); two right calcanei (NKT-153, NKT-268); four left metatarsals (NKT-133, NKT-136, NKT-139, NKT-160); two right metatarsals (NKT-138, NKT-144); a distal part of a right metatarsal (NKT-151); three proximal parts of right metatarsals (NKT-132, NKT-140, NKT-168). The taxon is represented by at least four adult and a possibly young individual. Measurements are provided in Appendix 2: Tables 8-14.

**Cranium (NKT-172).** The cranium is badly crashed, moderately deformed, and laterally compressed (Fig. 7). It preserves both toothrows but in the left one the molars are very badly preserved (Fig. 7C). The mesial margin of the orbit reaches the level of $M^3$. The length from the mesial edge of the orbit to the mesial root of $P^2$ is 154 mm. A pair of supraorbital ossicones is present, both broken near the base (Fig. 7A). It can be assumed that the ossicones are placed relatively medially compared to the dorso-lateral orbital margins, although the


FIG. 8. — *Palaeotragus* aff. *berislavicus* from Nikiti-1, Chalkidiki peninsula, Greece (latest Vallesian): **A**, radius, LGPUT NKT-156; **B**, radius, LGPUT NKT-155; **C**, metacarpal III-IV, LGPUT NKT-137; **D**, metacarpal III-IV, LGPUT NKT-131. Views: **1**, proximal; **2**, cranial (dorsal); **3**, distal; **4**, caudal (palmar) views. Scale bar: 20 cm.

skull is very deformed. The basal anteroposterior diameter of the ossicones is 43.4 mm, while the transverse diameter is *c.* 32 mm. Their cross section is oval shaped with main axis trending anteroposteriorly.

**Upper dentition**. The labial side of the left molars of NKT-172 is damaged (Fig. 7C; Table 8). The toothrows are not very worn. The $P^2$ and $P^3$ have a circular occlusal outline. Labially, the parastyle and the paracone ribs are well-developed, whereas the metastyle is weak. The fossettes of the $P^2$ and the $P^3$ are wide and U-shaped. A hypoconal fold can be seen in the distal part of the $P^3$'s fossette. Compared to the $P^2$ and $P^3$, the $P^4$ has a more pronounced metastyle, and a less convex lingual wall giving to it a more squared occlusal outline. The central fossette of the $P^4$ is wide and simple. On the disto-lingual part of the $P^4$ there is a style that reaches almost to the half of the crown height.

The basic morphology of the molars is similar to those of other giraffids (Fig. 7C). The $M^2$ and $M^3$ are slightly worn and have well-developed parastyle, paracone rib, mesostyle and metastyle. The labial rib of the metacone is almost flat. A weak labial cingulum is present on $M^1$ and $M^2$. On the $M^3$ a labial style is attached on the basis of the metacone. Lingually, the protocone and the hypocone are almost equally prominent and of similar shape on the $M^1$ and $M^2$. In the $M^3$ the protocone protrudes lingually more than the hypocone. The distal protocone and mesial hypocone flanges converge in the middle of the tooth. The distal hypocone flange tends to connect with the metastyle; they are already connected in the less worn $M^3$. The size of the mesial fossette is small. Mesially, the protocone flange is connected to the parastyle. Both fossettes are U-shaped. There is a very weak hypoconal fold in the $M^2$.

**Postcranials**. The preserved distal humerus (NKT-161) is crashed and deformed preventing reliable morphological observations (breadth of distal epiphysis: 85.4 mm; width of distal epiphysis: 40.94 mm). Its size is intermediate between those of *P. rouenii* and *P. coelophrys*. It has the same width as a *P. microdon* specimen described by Bohlin (1926). On the NKT specimen, the olecranon fossa is deep, wide and U-shaped.

The radii are all elongated (Fig. 8A, B) and moderately slender. Two of the NKT radii are fairly curved (concave laterally; NKT-155, NKT-156; Fig. 8A, B; Table 9), while the rest three are straighter (NKT-159, NKT-167, NKT-169). The cross section is crescent-shaped in the proximal ⅘ of bone's length, with rounded cranial and straight caudal faces; it is trapezoidal shaped in the distal most ⅕ of radius length. The two epiphyseal areas are both much wider than the shaft, and they both expand medially and laterally. In the specimen NKT-159 the olecranon is partly preserved. It seems to greatly tilt latero-distally. Proximally, the medial, rectangular/subrectangular shaped articular surface is much larger than the quadrangular lateral one, separated by each other by a wide, shallow furrow (Fig. 8A1, B1). The medial tuberosity is not


FIG. 9. — *Palaeotragus* aff. *berislavicus* from Nikiti-1, Chalkidiki peninsula, Greece (latest Vallesian): tibia, LGPUT NKT-271 in: **A**, proximal; **B**, cranial; **C**, distal, **D**, caudal views. Scale bar: 20 cm.

developed. A tilted narrow crest divides the distal articular surface into two equal subregions, representing the articular surfaces for the scaphoideum and semilunare, respectively. They are both round and slightly concave. The semilunare surface is interrupted by a convex protrusion distally. The groove for the extensor carpi radialis muscle at the cranial part of the distal epiphysis is wide, and very shallow to flattened, delimited by blunt ridges (Fig. 8A2, B2).

The best preserved metacarpals (Fig. 8C, D) vary slightly in length (Table 10), having however similar robusticity indices (8.38-8.75%). The lateral and medial epicondyles are asymmetrical. The lateral epicondyle has half the size of the medial one, and it is of square or rectangular shape. The medial epicondyle is rounded dorsally and has an overall shape of a half to ¼ of a circle. The fossa in-between the two epicondyles continues in the medial epicondyle. The medial and lateral epicondyles continue to the medial and lateral ridges respectively, which are of similar width and morphology. They are both rounded near the proximal end and they become slenderer and sharper in the shaft area. The central trough is very deep near the proximal end of the bone but becomes shallower and flatter towards the distal end. The trough's width is variable. However, it can be said that the longer the bone, the wider is the trough. The pyramidal rise is absent in most of the specimens apart of NKT-137 in which a slight protrusion could be attributed to the pyramidal rise; however, it is not prominent at all. The keels of the distal epicondyles are more prominent palmary, and they also extend onto the distal end of the palmar side of the shaft.

Three tibia specimens are preserved (Table 11). Proximally, the angle of the sulcus mascularis is obtuse when compared to the bovid or cervid anatomy (Fig. 9A, B). The tuberosity is not well preserved but does not seem to be pronounced (Fig. 9). The lateral condyle is somewhat damaged laterally and cranially. In the better preserved distal tibial fragment NKT-154 the cross section of the distal shaft is sub-rectangular. The distal articular surface has a broad rectangular shape, and the articular surface for the medial malleolus is quite prominent (Fig. 9C). The cochlear crest, that separates the cochlear furrows, is moderately prominent forming a strong caudal and a weak cranial crest.

The size of the three preserved NKT astragali (Fig. 10; Table 12) is intermediate between the groups of small and large *Palaeotragus.* The NKT astragali are rectangular in shape, as the lateral and medial lengths are of almost equal size and not thickened medially. In dorsal view the lateral edge of the trochlea tilts slightly medially. The central fossa is large, deep and triangular. The medial groove is weak in NKT-266; it is damaged in the other two specimens. The lateral notch is faint in NKT-266, prominent in NKT 267 (Fig. 10A) and intermediate in NKT-163 (Fig. 10B). The median depression is wide and deep in NKT-163 and NKT-266 but shallower in NKT-267. Ventrally, the medial ridge tilts medially in the specimens NKT-266 and NKT-267 (Fig. 10A), while it is almost vertical in NKT-163 (Fig. 10B). The intertrochlear notch is deep and narrow in NKT-163, but it is wide and shallow in NKT-266 and NKT-267 (Fig. 10). The proximal triangular fossa is prominent and the interarticular groove absent in all the specimens. The medial scala is absent in NKT-267, weak in NKT-266 (Fig. 10A) and slightly more prominent in NKT-163 (Fig. 10B). The distal intracephalic fossa is absent in NKT-266

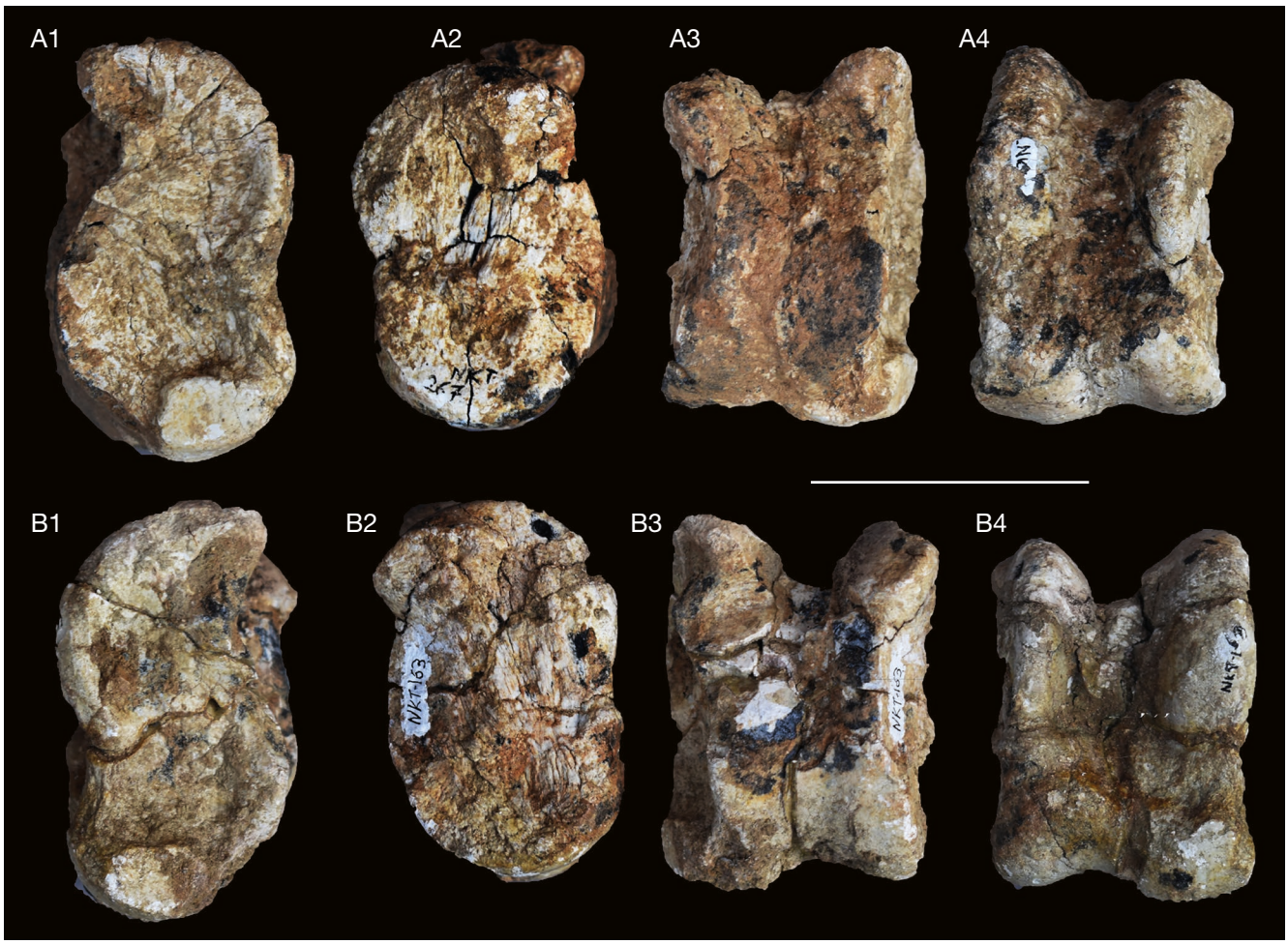


Fig. 10. — *Palaeotragus* aff. *berislavicus* from Nikiti-1, Chalkidiki peninsula, Greece (latest Vallesian): **A**, astragalus, LGPUT NKT-267; **B**, astragalus, LGPUT NKT-163. Views: **1**, lateral; **2**, medial; **3**, posterior; **4**, anterior. Scale bar: 5 cm.

and NKT-267; in NKT-163 it probably exists, although the preservation status of the specimen does not allow to be decisive (Fig. 10). The lateral and medial crests are equally thick, with the lateral pointing posteriorly, and the medial slightly tilting medially. The lateral side of the astragali is somewhat concave.

Two right calcanei were collected. The calcaneus NKT-153 (Fig. 11; Table 13) is larger, with a more robust corpus than NKT-268. However, the NKT-268 head seems to be stronger relatively to the corpus, than the NKT-153 one. Both the dorsal and plantar crests are parallel to the bone axis. The calcaneal tuberosity is prominent, though weathered in both specimens. In NKT-268 a medial crest separates the calcaneal tuberosity from the rest of the calcaneal corpus. The sustentaculum tali is somewhat damaged in NKT-153 (Fig. 10B, C), while it is robust in NKT-268. The proximal-plantar articular surface for the astragalus consists of two concave surfaces, with the plantar one being almost double in size than the dorsal surface. Medially, the articular surface for the astragalus is fairly deep and concave. The articular surface for the scaphocuboideum is located plantarly and is slightly damaged in both specimens. Dorsally, there is a well-developed, articular facet for the malleolus.

The metatarsals (Fig. 12; Table 14) demonstrate a variation in both the total length and the robusticity indices (7.3-12%), also partly due to postmortem deformation (e.g., NKT-133). The lateral epicondyle is smaller and subdivided in two regions, the dorsal and the plantar heads (Fig. 12A). In contrast, in the medial proximal epicondyle this separation is not evident. The medial epicondyle has a trapezoid shape (Fig. 12A). The lateral dorsal head is more circular. The shape of the lateral plantar head is intermediate in shape. The pygmaios is not preserved (Fig. 12A, B). The central trough varies in the studied specimens. However, it is significantly shallower and it disappears from the middle towards the distal end of the bone (Fig. 12B). The width of the trough also varies, and it seems to follow the total bone width. The proximo-plantar fossa is present, weak and communicates with the central trough in the specimen NKT-139 whereas the bad conservation status of the other specimens does not allow to identify it. In contrast to the metacarpals, a dorsal trough is evident; it is deeper at the proximal end of the bone, becomes shallower downwards and disappears at the distal end (Fig. 12D). The distal epiphysis of the metatarsals is similar to that of the metacarpals.

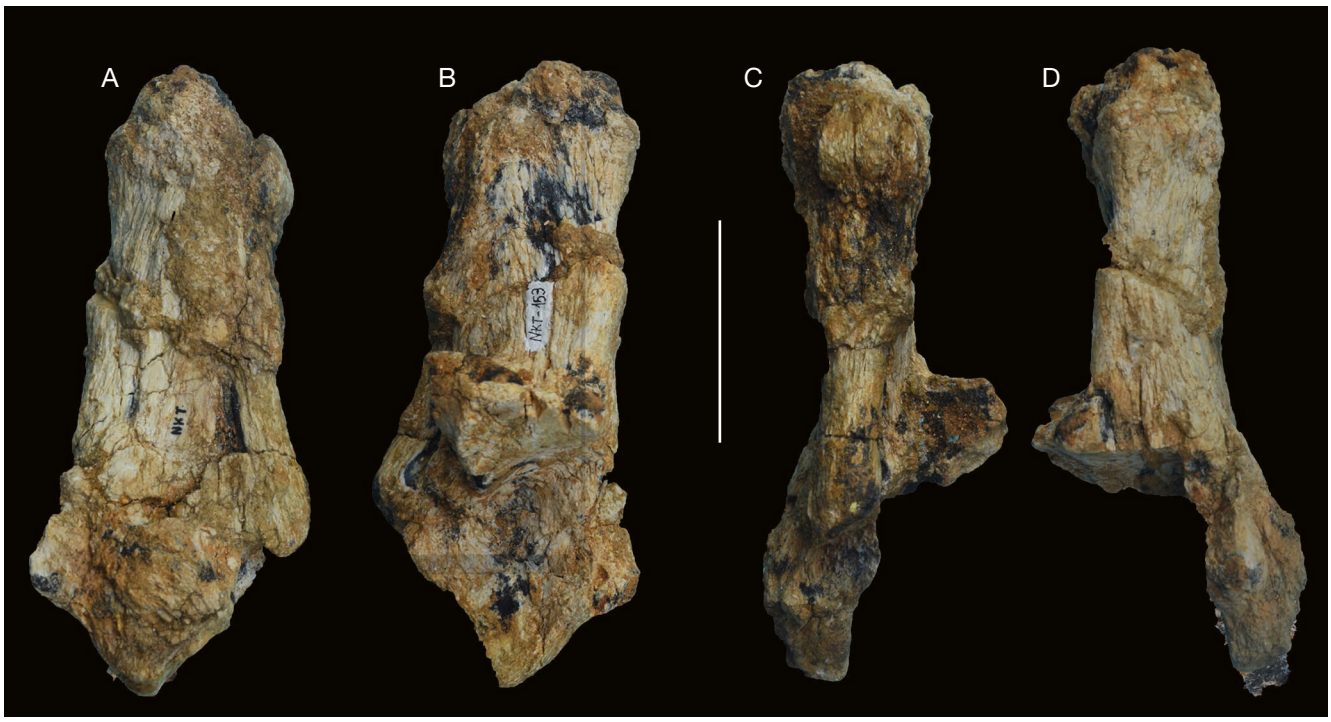


Fig. 11. — *Palaeotragus* aff. *berislavicus* from Nikiti-1, Chalkidiki peninsula, Greece (latest Vallesian). Calcaneus, LGPUT NKT-153 in: **A**, lateral; **B**, medial; **C**, dorsal; **D**, plantar views. Scale bar: 5 cm.


Fig. 12. — *Palaeotragus* aff. *berislavicus* from Nikiti-1, Chalkidiki peninsula, Greece (latest Vallesian). Metatarsal, LGPUT NKT-136 in: **A**, proximal; **B**, plantar; **C**, distal; **D**, dorsal views. Scale bar: 20 cm.

## COMPARISON

### *The taxonomy of Late Vallesian Eurasian Palaeotragus*

Assessing the relationships among the Late Miocene *Palaeotragus* taxa is a difficult task. A variety of species were described in the late 19th and early 20th centuries, in a time when communication among different scholars was quite difficult. Since then, just a few comprehensive systematic revisions have been accomplished (e.g., Godina 1979; Geraads 1986), even though the genus is the most common giraffid in the Late Miocene of Eurasia. The problem is further exacerbated by the wide geographical distribution of the relevant samples and their usually fragmentary nature.

Traditionally, *Palaeotragus* species are distinguished by means of size in two groups (Geraads 1974, 1986; Iliopoulos 2003; Kostopoulos & Saraç 2005; Kostopoulos 2009). The first group usually includes the small-sized taxa *Palaeotragus rouenii, P. microdon* and sometimes *P. pavlowae.* The term *"P. rouenii* group" is generally used for this ensemble of taxa, characterized by their small size and their long, slender metapodials. The second group incorporates larger species such as *Palaeotragus coelophrys, P. quadricornis, P. expectans, P. borissiaki, P. hoffstetteri, P. moldavicus, P. asiaticus* and *P. berislavicus.* The name *"P. coelophrys* group" is usually applied for larger-sized members, which are also characterized by the shorter and more robust metapodials than those of the "*P. rouenii* group". Earlier works by Geraads (1974, 1986), do not detect any

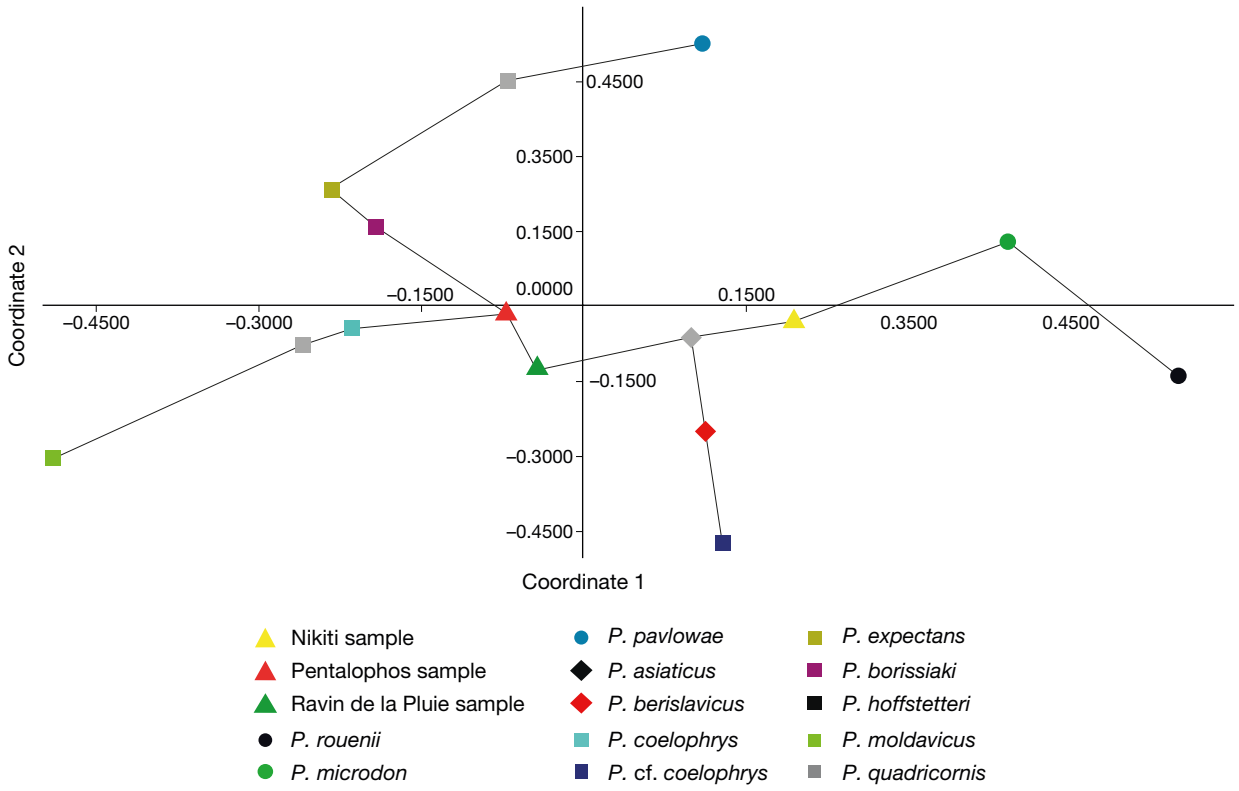


FIG. 13. — Principal Coordinates Analysis (plane of coordinates 1 and 2, representing 39,5% and 15,3% of initial data variance) comparing 27 biometrical variables and 4 selected features of premolar morphology of the Late Miocene Eurasian palaeotrages, as well as the Vallesian Greek *Palaeotragus* Gaudry, 1861 samples studied here.

significant or consistent morphometric difference among members of the *"P. coelophrys* group", and all these taxa are commonly treated as possible synonyms under *P. coelophrys,* although the same author (Geraads *et al.* 2013) recently recognized the need for a deeper revision.

Godina (1979) on the other hand, followed a quite different approach, recognizing all species known at that time (except *P. quadricornis*) and grouping them into three distinct subgenera: *Palaeotragus* (*Palaeotragus*), with *P. rouenii* and *P. pavlowae*; *Palaeotragus* (*Yuorlovia*), with *P. coelophrys, P. microdon, P. asiaticus* and *P. hoffstetteri*; and *Palaeotragus (Achtiaria),* with *P. expectans, P. borissiaki, P. moldavicus* and *P. berislavicus.* According to Godina (1979) representatives of *Achtiaria* differ from those of *Yuorlovia* by a shorter cranial face, a shorter diastema compared to the toothrow length and a non-continuous lingual wall on the $P_3$. Members of *Palaeotragus* are smaller in size, the front part of the skull is elongated, and the diastema length exceeds that of the toothrow; the lingual wall of $P_3$ could be either continuous or not.

Godina's (1979) taxonomic point of view has not been widely accepted and is proving quite fragile in several respects. First, the type material of most species in question does not include the anatomical elements on which presumed taxonomic distinctions are based. Additionally, the validity of most diagnostic features is challenged by the scarcity of the material. For example, while Godina (1979) repeatedly used mandibular characters to assess similarity, for some of the proposed species only a single mandibular specimen was known at that time per species, while for some others there were not even complete mandibular specimens preserved. The morphology of the ossicones used to distinguish some of the bulky palaeotrages by Godina, was not known for all *Palaeotragus* species (e.g., *P. coelophrys* from Maragheh), whereas sexual dimorphism proved later to have a strong effect on the ossicone size (e.g., Geraads 1978; Kostopoulos 2009).

To test previous taxonomic assumptions, we perform here an analysis of 27 available biometrical variables (absolute and relative) and of 4 selected morphological characters of premolar morphology (see Appendix 1). In order to avoid discrepancies per species introduced by later assignments our initial analysis was based exclusively on the material provided from the type localities. Our basic results are summarized and better illustrated by a PCO analysis (Fig. 13) on which the Greek material studied here is also extrapolated (see Appendices 3, 4 for additional information). All multivariate treatments of both PCA and PCO suggest the following clusters:

*P. microdon* and *P. rouenii* are always separated from the rest of taxa, as well as between them, keeping a marginal position on the diagrams (Fig. 13; Appendix 3: Figs S1, S2).

*P. berislavicus*, *P. asiaticus* and the Nikiti-1 taxon are grouped more closely together than with other compared taxa. PCO analyses constantly indicate *P.* cf. *coelophrys* from China as closer to this set of taxa, though in PCA the Chinese species appears isolated.

*P. coelophrys* from Maragheh, *P. borissiaki*, and *P. expectans*, along with PNT and RPl samples are grouped closer together than to other taxa. *P. quadricornis* from Samos and the Sinap *P. hoffstetteri* always appear closer to members of this group than to the previous one. The same may apply for *P. moldavicus*, though this taxon appears in several analyses more distant.

*P. pavlowae* is the most debatable taxon among the compared ones but also one of the less known. It appears close to *P. asiaticus-P. berislavicus*-NKT ensemble in PCA, but it is quite remote in PCO.

The taxonomy of *P. rouenii* and *P. microdon* is sufficiently solid. Both taxa represent the smaller Late Miocene representatives of the genus with the Chinese taxon, *P. microdon* being distinguished from the European one, *P. rouenii* by its longer toothrow with shorter premolars compared to molars, more advanced $P_3$, shorter and more robust radius and metacarpal and shorter but equally slender metatarsal (Appendices 3, 4; see also Bohlin 1926; Geraads 1974; Hamilton 1978; Kostopoulos & Saraç 2005). Among several populations of *P. rouenii* described so far, three are worthy of further mention. First, the *P. rouenii* sample from Thermopigi (Xafis *et al.* 2019) demonstrates extremely elongated postcranials, especially the radius (SIT-939), and metatarsal (SIT-307; Xafis *et al.* 2019). A similarly long radius has been described by Kostopoulos & Koufos (2006) from Perivolaki (LGPUT PER-1180), whereas two very long metatarsals (but shorter than those from Thermopigi) have been described from Kryopigi (LGPUT KRY-7937, KRY-7938; Lazaridis 2015). Although the extreme lengthening of these specimens cannot be easily interpreted, it is certainly indicative of the strong dolichopodiality developed in some *P. rouenii* populations, allowing an overall re-consideration of its intraspecific metrical variability.

*P. pavlowae* was erected by Godina (1979) based on material from Grebeniki (Ukraine) originally described by Pavlow (1913) as *Camelopardalis parva*. Pavlow (1913) ascribed to this taxon only a palate (RSGU 1637) and referred to the same genus a $M_2$-$M_3$ (no catalogue number indicated). Godina (1979) uses RSGU 1637 as the holotype of *P. pavlowae* and also refers to this species an upper and a lower juvenile dentition (OSU 2376 and OSU 2375, respectively), a partial ulna, and an astragalus (OSU 2749, OSU 2746, respectively) stored in the Odessa Museum, a first phalanx (SIZK 25-118) stored in Kiev, all from Grebeniki as well as an upper $P^2$-$M^3$ (RSGU 1639) from Blagodarnenskaya, Stavropol. No lower dentition has been ascribed to *P. pavlowae* from its type locality. Godina's (1979: 44) poor species diagnosis indicates: "*Length $P^2$-$M^3$ – 127 mm. Limbs of intermediate length and massiveness*" (translated from Russian). The length of the holotype upper toothrow from Grebeniki is indeed larger than that of *P. rouenii* (Appendices 3, 4) and within the metrical and proportional range of *P. microdon*. On the other hand, the postcranials ascribed by Godina (1979) to this taxon appear larger and more robust than those referred by Bohlin (1926) to *P. microdon* and are closer to those from Pavlodar [a metatarsal (PIN 2432/7005) and three astragali (PIN 2346-130, PIN 2346-151, PIN 2413-6939)] referred to as *P. asiaticus* (Appendices 3, 4). The deciduous upper dentition from Grebeniki assigned to the same species is comparable in size to that of *P. rouenii* ($dP^2$-$dP^4$ average length= 57 mm), but the milk teeth show a well-developed lingual cingulum; the $dP^2$ is more symmetric mesio-buccally; the mesial lobe of $dP^3$ is rather triangular than trapezoidal, the angle formed by the mesial and distal buccal flanges of the paracone is obtuse, and the mesio-buccal stylid is bifurcated; a postprotocrista and a neocrista are still detectable on the $dP_3$; as the $dP_4$, $M^1$ and $M^2$ show a strong hypoconal spur (pers. obs.; unfortunately, we couldn't locate OSU 2375 in the Odessa collections). By these features OSU 2376 appears closer to the dental morphology of AMNH 22807 from Samos and AMNH 26362 from Shansi (see Kostopoulos 2009:308), as well as to *P. expectans* (see Borissiak 1914: pls 1, 2). Inadequate evidence does not allow definitive conclusions about the Grebeniki taxon; we consider it more likely to be a chimeric species resulting from the mixing *P. rouenii* material with that of another palaeotrage.

Two morphometric clusters are recognized here within the group of large Late Miocene palaeotrages. *P. coelophrys, P. expectans, P. borissiaki,* and *P. quadricornis* share a more primitive $dP_3$ and $P_3$ structure (the former unknown in *P. quadricornis*), larger size and more robust proportions compared to the rest of the examined taxa. The $dP_3/P_3$ morphology and postcranial proportions of *P. hoffstetteri* are very similar to this group of taxa, as deduced from several postcranials in MNHN, Paris and NHM Izmir (most of them belonging to the original material described by Ozansoy in 1965) and some dental remains from Loc 49 of Sinap (referred to as *P. coelophrys* by Gentry 2003). As others before us (e.g., Churcher 1970; Geraads 1974, 1978) we think that there are no sufficient ground to discriminate within this set of taxa, for which we apply by priority the name *P. coelophrys*. By its absolute dimensions and proportions *P. moldavicus* matches pretty well *P. expectans-P. borissiaki* but differs in apparently fully molarized $P_3$ of the paratype mandible PIN 649/26 (Godina 1979: fig. 8). Moreover, *P. moldavicus* postcranials appear to be larger than those of other members of this group. However, the known material is so scarce, that any attempt to distinguish it from other large palaeotrages would be premature at the moment.

The second group of large Late Miocene palaeotrages recognized in our analysis includes *P. berislavicus* and *P. asiaticus*. They share a fully molarized $P_3$, dental proportions and limb lengths comparable to those of *P. rouenii*, but the dentition is significantly larger (*c.* 15%) and the postcranials stouter, though not as much as in *P. coelophrys* (Appendices 3, 4). Although suggestions about the Vallesian *P. berislavicus* morphology and proportions are relatively safe as they are based on material from a single locality, Berislav (Ukraine), the younger *P. asiaticus* is a more doubtful species. The Ortok (Kyrgyzstan) type material (Godina 1979) includes a cranium with toothrow and a $P^2$-$P^4$ both intermediate in size and premolar/molar proportions between *P. rouenii/P. microdon* and *P. coelophrys* (Appendices 3, 4); a few isolated upper and lower teeth with some approaching better *P. coelophrys*, while others being closer to the upper range of *P. rouenii/P. microdon*; a radius similar in size and proportions to *P. coelophrys* (Appendix 3: Fig. S5); two

intermediate tibiae (Appendix 3: Fig. S7); and an astragalus comparable in size to *P. rouenii* (Appendix 3: Fig. S8). No metapodials are known from the type locality. Material from Pavlodar (Kazakhstan) ascribed by Godina (1975, 1979) to the same species includes some isolated lower teeth intermediate in size but closer to *P. coelophrys*; a metatarsal as long as that of *P. rouenii* but more robust (Appendix 3: Fig. S9); and three astragali similar to those of *P. coelophrys* (Appendix 3: Fig. S8). An intermediate in size lower dentition (length $P_2$-$M_3$=141 mm) and a metatarsal as long as in *P. rouenii* (453 mm) from Kalmakpaj (Kazakhstan), as well as a partial metatarsal from Pristashkent district (Uzbekistan) were also ascribed to *P. asiaticus* by Godina (1979). Although we cannot fully exclude the possibility that *P. asiaticus* may represent a distinct taxon, similar in several respects to *P. berislavicus*, it is also highly probable that the species concept is based on a mixture of material of two different species.

By its toothrow size *P.* cf. *coelophrys* from China matches pretty well the *P. berislavicus-P. asiaticus* ensemble. Its $P_3$ is also molarized (Bohlin 1926: pl. 3), but the hypoconulid is communicating with the mesial lobe of the tooth. The only postcranial evidence available for this taxon is an astragalus (Bohlin 1926 – Appendices 3, 4), whose proportions do not differ from those of *P. rouenii*, or *P. berislavicus-P. asiaticus*. The Chinese taxon could actually belong to the same species represented by the roughly contemporaneous and geographically close Ortok-Pavlodar samples, a hypothesis already proposed by Godina (1975, 1979). For the time being and until new material is available we prefer to exclude the Asian taxa from our overall concept and we consider *P. berislavicus* as a valid species based on the Berislav material only.

*Conclusion*

To sum up, our overview of the Late Miocene palaeotrages from Eurasia allows recognizing four valid species

*P. rouenii* Gaudry, 1861; type species characterized by small size, fairly molarized $P_3$/$dP_3$, lower premolar to molar length ratio between 57% and 62%, and strongly dolichopodial limbs. Female ossicones absent or very slim.

*P. microdon* (Koken, 1885); characterized by small size, longer toothrow with shorter premolars (lower premolar to molar length ratio between 63% and 73%), more advanced $P_3$, shorter and more robust radius and metacarpal and shorter metatarsal than the type species. Females bear slender ossicones.

*P. berislavicus* Korotkevitch, 1957 (possible synonym of *P. asiaticus*); characterized by intermediate size, fully molarized $P_3$, and similarly long but stouter limbs than the type species.

*P. coelophrys* (Rodler & Weithofer, 1890) (synonym of *P. expectans, P. borissiaki, P. hoffstetteri, P. quadricornis,* and possible synonym of *P. moldavicus*); characterized by larger size, less molarized $P_3$/$dP_3$, and more robust limbs than the type and rest of species. Known females lack ossicones.

## *The Vallesian Greek large palaeotrages*

*Pentalophos sample*

The dental remains from Pentalophos indicate a taxon significantly larger than *P. rouenii*, and *P. microdon*. In most absolute size and proportions, they match those of *P. coelophrys* (Fig. 13; Appendix 3). Comparing the PNT upper teeth with those of the type cranium of *P. coelophrys* from Maragheh, premolars have in both cases a slight hypoconal fold but the $P^2$ from Maragheh has a somewhat prominent lingual rib in the hypocone area that it is absent from the $P^2$ of PNT. The $P^3$ of Maragheh is similar to that of PNT, except that it is squarer and bears a lingual groove. In the only available $P^4$ from PNT, the paracone is more centrally placed, the $P^4$ fossette is somewhat better developed mesially and lingually, and the occlusal outline more triangularly shaped than in Maragheh. The premolars of the Vallesian *Palaeotragus* from Sinap illustrated by Ozansoy (1965: pl. X, fig. 3) resemble a lot that of PNT, although they are significantly more square (especially the $P^4$) and with enlarged fossettes. The premolars of another Sinap upper toothrow housed in MNHN Paris (MNHN.F.TRQ no catalogue number) show a much weaker hypoconal spur and a more robust paracone, while the parastyle is considerably weaker in $P^2$ and $P^3$ compared to the PNT premolars. Finally, the $P^4$ is squared in the MNHN.F-Sinap specimen, in contrast to the triangular $P^4$ from PNT. The Vallesian *P. coelophrys* from Eldari (Alexeev 1930: pl. I, figs 1-4) bears an unusually triangular $P^3$ (specimen PIN 1408/381), while the $P^3$ of the specimen PIN 1408/202 is identical to the premolars of PNT, probably bearing a prominent distolabial stylid, similar to that of the $P^2$ of PNT-113. The $P^4$ has a circular occlusal outline in PIN 1408/381 and squared in PIN 1408/202, in contrast to the triangular in PNT-113. The lower deciduous dentition from Pentalophos (LGPUT PNT 121F) is almost identical to that of the Vallesian *P. coelophrys* from Sebastopol (Borissiak 1914: pl. II, figs 1-5), both having a large rhomboid mesial lobe and strong ectostylids on $dP_4$ and a less advanced $dP_3$ with the metaconid being attached to the protoconid-entoconid junction and turned strongly forwards without closing the anterior valley.

The PNT metatarsals seem to approach better *P. coelophrys*, as they are considerably robust proximally (Appendix 3: Fig. S9). The morphology of the proximal articular surface of PNT differs from that of *P. rouenii* in the bone protrusion instead of light groove separating medially the plantar and dorsal heads, the non-tilt plantar head, the more robust lateral dorsal head, and the less prominent pygmaios.

Multivariate analysis (Fig. 13; Appendix 3) consistently suggests PNT taxon as grouped with the largest palaeotrages. Hence, according to both morphological and metrical evidence we attribute the Pentalophos taxon to *P. coelophrys*.

*Ravin de la Pluie sample*

Geraads (1978) originally studied the RPl-91B cranium and referred it to as *Palaeotragus* cf. *coelophrys.* A new morphological comparison of the worn toothrows, indicates that the RPl palaeotrage has more rectangularly shaped and larger premolars compared to molars than the *P. coelophrys* type from Maragheh, The $P^3$ and $P^4$ of RPl are very similar in shape with the $P^3$ and $P^4$ from the Vallesian specimen PIN 1408/202 of *P. coelophrys* of Eldari (Borissiak 1914: pl. I, fig. 4). They are also very similar with the teeth of the Vallesian *P. coe-*

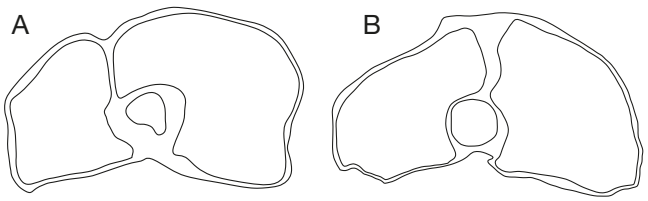


Fig. 14. — Morphological comparison of *Palaeotragus* Gaudry, 1861 proximal left metacarpal epiphyses: **A**, *P. rouenii* Gaudry, 1861 from Nikiti-2; **B**, *P.* aff. *berislavicus* from Nikiti-1.

*lophrys* from Sinap (MNHN.F.TRQ no catalogue number), although more square shaped. Most likely due to advanced wear, the paracone of the $P^3$ and $P^4$ of the RPl skull is much less prominent than the paracone of the respective teeth of the MNHN.F specimen. The premolars of the *P. coelophrys* specimen from Sinap, provided by Ozansoy (1965: pl. X, figs 1-3), are almost identical to those of the RPl, in both shape and morphology. However, the fossettes of the Sinap specimen are slightly larger, likely due to the less advanced wear stage. Although the labial ribs of the RPl molars appear less prominent than those of PNT (but different wear stage may again exaggerate differences) both samples are placed close in the PCO analysis (Fig. 13) and within the range delineated by taxa included herein into *P. coelophrys* (see also Appendix 3: Figs S1-S4).

According to our observations and measurements the RPl taxon fits better *P. coelophrys* than any other taxon recognized herein. In fact, RPl's cranium has one of the largest described toothrows. The absence of any postcranial material from that site prohibits any further comparison. Hence, we just confirm Geraads (1978) classification of that material as *Palaeotragus* cf. *coelophrys.*

*Xirochori sample*

The size of the single specimen from Xirochori approaches the mean values of *P. coelophrys* (Appendix 3: Fig. S11). Although the Xirochori molars are less worn, their morphology is almost identical to that of RPl, from which it differs in having a less distally pointed third lobe of the $M_3$. In any case the material is inadequate for certain conclusions and it is therefore referred to as *Palaeotragus* sp.

*Nikiti-1 sample*

The cranium and associated upper dentition from Nikiti-1 are significantly larger than those of *P. rouenii* and *P. microdon* and within the size range of *P. coelophrys – P. berislavicus – P. asiaticus*. The poor preservation status of NKT's skull does not allow for an extended comparison with *P. coelophrys* holotype from Maragheh and the two specimens belong to different sexes possibly exaggerating differences.

Dentally, the upper toothrow from NKT differs from that of PNT (and RPl to the extent that morphologies can be recognized due to advanced wear) in the weaker styles (especially the metastyle) of the premolars, the less protruding paracone rib of the more squared $P^4$, and the even weaker metacone rib of the molars. Compared to *P. berislavicus* holotype (Korotkevich 1957), the labial ribs are equally developed in both samples. However, the $P^2$ and $P^3$ of the Berislav giraffid are circular, while the same teeth from NKT are more square shaped. *P. berislavicus* demonstrates a triangular $P^4$, while *Palaeotragus* from NKT has a square $P^4$. Moreover, the $P^4$ from NKT bears a lingual stylid that is missing from *P. berislavicus.*

In spite the bad preservation of most NKT postcranials, they clearly indicate a taxon proportionally close to *P. rouenii* though slightly more robust and with shorter metapodials. The NKT radius falls into the lower length range of *P. rouenii* (Appendix 3: Fig. S5) but it has a broader distal part. In that feature it agrees with *P. berislavicus* and *P. asiaticus* (Appendices 3, 4) although there is only one radius specimen available for each of these two taxa. In five complete radii of *P. rouenii* from several sites (except Kemiklitepe D, Turkey), the robusticity index (DT diaphysis/Length) is always below 10; it ranges between 10.4 and 11.2 in the four radii from NKT and between 10 and 13 in *P. coelophrys-P. berislavicus-P. asiaticus* (n=5). Unfortunately, data on the cranio-caudal diameter of radius are very limited. However, some scarce measurements (Geraads 1974), seems to indicate that *P. rouenii* had a significantly slenderer radius than NKT, at least proximally. In fact, the cranio-caudal diameter of NKT's radius is closer to that reported for *P. coelophrys.* However, when NKT specimens are compared with some *P. rouenii* radii from the sites Perivolaki and Nikiti-2, they did not seem to be more robust proximally. The radius curvature is a feature which also varies among the NKT sample, as well as among *P. rouenii.* Shafts' cross section is of similar crescent shape. Distally and cranially, the V-shaped formation for the adhesion of extensor carpi radialis muscle is equally prominent in NKT and *P. rouenii*. The distal articular surface is also very similar in the NKT palaeotrage and *P. rouenii.*

For a similar length (= 395 mm at average, excluding the likely young-adult NKT-137) the metacarpals of *P. coelophrys* appear significantly more robust (RI *c.* 12 instead of 9.5 in NKT), whereas for a similar robusticity (9.5) the metacarpals of *P. rouenii* are usually significantly longer (>430 mm in 8 out of 12 specimens from several sites) than in NKT. Concerning the morphology of the metacarpals, there are several differences between the NKT taxon and *P. rouenii* (Fig. 14). Proximally, the bone protrusion which separates the medial and lateral epicondyles is much more intense in *P. rouenii* than in NKT. Moreover, the medial epicondyle is of trapezoidal shape and the lateral epicondyle is of square shape in *P. rouenii,* while they are both of half-circle shape in NKT. As a result, the proximal articular surface has a trapezoidal shape in *P. rouenii* and a half-circle shape in the NKT specimens. Dorsally, the shaft is parallel to the bone axis medially, while the axis of the bone and the shaft are angled laterally in *P. rouenii*. That feature is very prominent proximally and it could be said that the cross section of the shaft has a shape of a right triangle. The same feature exists in NKT's metacarpals too, although it is much less

prominent, and as a result, the cross section of the shaft is more rectangular. Palmary, the central trough extends throughout the whole bone in *P. rouenii* reaching at the trochlear, although it is considerably shallower distally than proximally. On the contrary, in the NKT metacarpals, the central trough seems to disappear at the distal ⅓ of the bone. Thus, the distal and palmar side of the metacarpal is completely flat in NKT. Distally the lateral condyle, seems to extend slightly more laterally in *P. rouenii* than in the NKT metacarpal. Finally, distally and dorsally, the shaft is somewhat more curved in *P. rouenii,* while in the NKT metacarpals is more flattened.

The tibia data are quite rare. According to the only fully preserved tibia available from NKT, its length falls within the *P. rouenii* range. However, it seems that the NKT taxon has broader distal epiphysis than *P. rouenii,* approaching *P. berislavicus* and *P. asiaticus* (Appendix 3: Fig. S7).

The NKT astragali and calcanei are intermediate in size between those of *P. rouenii* and *P. coelophrys*; the astragalus of *P. rouenii* from Perivolaki (PER) is more elongated than the NKT one, having a more rectangular shape (more square in NKT). The two astragali referred to *P. berislavicus* are smaller than the NKT ones and cannot be separated from those of *P. rouenii* (Appendix 3: Fig. S8).

By their proportions the metatarsals from NKT are placed in between those of *P. rouenii* and *P. coelophrys*; they are as long as the shorter known samples of *P. rouenii* but as wide as the largest individuals of this species. By these features, they approach better the two known metatarsals of *P. berislavicus* (Appendix 3: Figs S9, S10, S12).

Concerning the metatarsal morphology, there are several differences between the NKT taxon and *P. rouenii* on the proximal epiphysis (Fig. 15). Medially, the proximal articular surface is continuous in *P. rouenii,* while in NKT it is separated by a groove at the point between the two heads. Hence, the two heads of the medial epicondyle are more strongly separated in NKT. The shape of the dorsal head of the lateral epicondyle is half-circular in both NKT and *P. rouenii,* but in NKT is much more elongated. Moreover, in NKT that head is placed at a more obtuse angle to the axis of the proximal articular surface. In contrast, in *P. rouenii,* it is placed parallel to the proximal articular surface axis. As a result, the lateral epicondyle is of equal or of greater width to the medial epicondyle in NKT than in *P. rouenii.* In the medial epicondyle, the highest point of the dorsal face is more medial in *P. rouenii.* The plantar head of the medial epicondyle is extended plantarly in *P. rouenii* and it tilts laterally, while in NKT it is less extended and tilts medially. Those two heads are separated by a slight medial groove that is more marked in *P. rouenii* than in NKT. The central trough seems to vary significantly among NKT specimens in terms of depth and width. Finally, the distal part, relatively to the shaft, is wider in NKT than in *P. rouenii.*

Two assumptions can be formulated about the NKT taxon. The first one could be that two populations of *Palaeotragus* were present in Nikiti-1: a population of *P. rouenii* represented exclusively by postcranials and with slightly shorter and more robust limbs than typically, and a population of a taxon close to *P. coelophrys* represented only by the partial cranium NKT-172. The case of coexistence of different *Palaeotragus* species in Greece is already well known (Iliopoulos 2003; Kostopoulos 2009). However, both the absence of any postcranial element from Nikiti that could be safely grouped with *P. coelophrys* and the proportional and morphological differences of the available postcranials from typical *P. rouenii* challenge this assumption. The homogeneity of the postcranial sample suggests a single medium sized *Palaeotragus* species, intermediate between *P. coelophrys* and *P. rouenii.* The combination of cranial and most of the postcranial evidence points to a population similar to *P. berislavicus,* though more data from both taxa are needed for definitive conclusions. Hence, we refer at the moment the NKT palaeotrage to *Palaeotragus* aff. *berislavicus.*

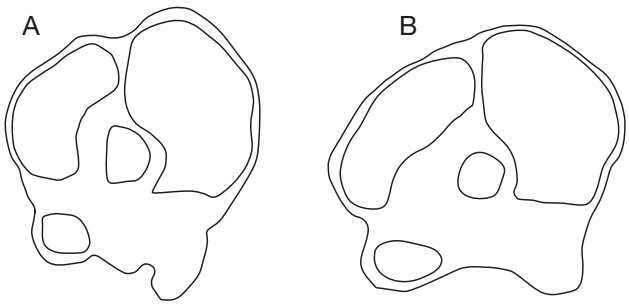


FIG. 15. — Morphological comparison of *Palaeotragus* Gaudry, 1861 proximal left metatarsal epiphyses: **A**, *P. rouenii* Gaudry, 1861 from Perivolaki; **B**, *P.* aff. *berislavicus* from Nikiti-1.

*THE TUROLIAN GREEK LARGE PALAEOTRAGES*

In our current knowledge large palaeotrages are relatively rare in the otherwise wealth Turolian faunas of Greece. Apart from the Samos Island (Kostopoulos 2009 and references therein) large *Palaeotragus* are reported from Kerassia (Euboea) and Thermopigi (Serres basin) sites (Iliopoulos 2003; Xafis *et al.* 2019). Samos material previously attributed to either *P. coelophrys* or *P. quadricornis* is herein considered as representing a single species, *P. coelophrys* (see also discussion in Kostopoulos 2009). Iliopoulos (2003) described two badly preserved mandibular fragments (K4/Δ8/1 and K4/Δ8/2) from Kerassia, most likely of the same individual, bearing $P_3$-$M_3$ right and $P_2$-part $P_4$ left, respectively. By its size and proportions (Lpm = 157.3 mm; Lp = 65.2 mm; Lm = 89.9 mm; data from Iliopoulos 2003), the Kerassia large palaeotrage fits within *P. coelophrys* and *P. berislavicus* size range. The rather advanced $P_3$ morphology and the relatively short molar row compared to the premolars might point to *P. berislavicus*, though material is not sufficient to provide any definitive determination.

Xafis *et al.* (2019) described from the Turolian fauna of Thermopigi (Greece) an upper premolar row, a left lower toothrow, an incisor and a canine as belonging to a larger palaeotrage than the well-documented *P. rouenii* from this site. Both the complete lower toothrow and the upper and lower

premolar row from Thermopigi are quite shorter than the larger palaeotrages recognized here (*P. coelophrys* and *P. berislavicus*; see Appendix 4). Metrically, the lower toothrow SIT 700 matches both *P.* cf. *coelophrys* from China and *P. asiaticus* from Kalmakpaj (Godina 1979, PIN 2432-84), whereas the $P_3$ shows similarly advanced molarization. Nevertheless, the Thermopigi specimens are just marginally longer or at the upper size range of *P. rouenii* and given the overall increased size (i.e., lengthening) of the local population of this species as indicated by the available postcranials, we could not exclude the possibility that those specimens may represent just a larger individual of *P. rouenii*.

## CONCLUSION

Our analysis confirms previous suggestions that morphometrical discrimination among *P. coelophrys*, *P. expectans, P. borissiaki, P. hoffstetteri, P. quadricornis* and possibly *P. moldavicus* is not sufficiently supported by present data, and hence all these taxa should be treated at the moment as possible synonyms under *P. coelophrys* (Rodler & Weithofer, 1890). Size differences between local samples (e.g., Maragheh vs. Starye Bogeny) might appear high in the light of extremely scarce evidence but they are not larger than size variance within the best recorded *P. rouenii* or other giraffid species (e.g., Ríos *et al.* 2016, 2017) The $dP_3/P_3$ molarization is usually less advanced in *P. coelophrys* than in *P. rouenii,* though morphological variation does exist and data are limited for statistically safe and definitive conclusions. Limb shortening and metapodial robusticity possibly increase from the Vallesian peri-Black Sea samples to the Turolian ones from Anatolia-Iran but the scarcity of the material does not allow to properly test this hypothesis.

In accordance with the Black Sea record, *P. coelophrys* appears to have a strong signal in the Vallesian faunas from Axios Valley, N. Greece, certainly recorded in Pentalophos and most probably in Ravin de la Pluie; the Xirochori mandible may also belong to the same species but material is insufficient. Turolian reports of the species in continental Greece are rather dubious but the taxon has a strong presence in contemporaneous faunas south of Caucasus from where probably expanded westwards in the Anatolian domain.

*Palaeotragus asiaticus* and *P.* cf. *coelophrys* from the Turolian equivalent of Central Asia (Kyrgyzstan, Uzbekistan, and Kazakhstan) and China respectively, are probably closely related to each other. They could represent an eastward offshoot of Iranian *P. coelophrys* or – as the biometric data suggest – they might originated from another taxon; in that case the Vallesian *P. berislavicus* from Ukraine would be an ideal ancestor by means of morphometry. The Berislav palaeotrage is placed morphometrically between *P. rouenii* and *P. coelophrys*, and it probably invaded Southern Balkans at the end of the Vallesian, documented in the Nikiti-1 fauna. It is also possible that the species survived here quite later, as the Kerassia record may imply, but data are once again inadequate for certain conclusions.

**Acknowledgements**
This work is based on the Master Thesis of the first author realized under the auspices of the Interinstitutional Program of Postgraduate Studies in Palaeontology-Geobiology directed by the School of Geology of the Aristotle University of Thessaloniki. Thanks are due to George Koufos, Louis de Bonis and all colleagues who contributed over the years to the excavations in Axios valley and Nikiti. We are also grateful to George Iliopoulos for sharing information and illustrations of several discussed specimens. Maria Ríos and George Iliopoulos are deeply thanked for valuable comments and suggestions.

## REFERENCES

Alexeev A. 1930. — Die obersarmatische Fauna von Eldar. *Travaux du Musée géologique près l'Académie des Sciences de l'URSS* 8: 167-204 (in Russian with German abstract).
Athanassiou A. 2014. — New giraffid (Artiodactyla) material from the Lower Pleistocene locality of Sésklo (SE Thessaly, Greece): Evidence for an extension of the genus *Palaeotragus* into the Pleistocene. *Zitteliana B* 32: 71-89. https://doi.org/10.5282/ubm/epub.22388
Bohlin B. 1926. — Die Familie Giraffidae. *Palaeontologia Sinica,* Series C. Volume 4 (1): 1-178.
Borissiak A. 1914. — Mammifères fossiles de Sébastopol II. *Mémoires du Comité géologique, St. Petersburg,* nouvelle série, 87: 105-154.
Churcher C. S. 1970. — Two new upper Miocene Giraffids from Fort Ternan, Kenya, East Africa. *Fossil Vertebrates of Africa* 2: 1-105.
Churcher C. S. 1978. — Giraffidae, *in* Maglio V.J. & Cooke H. B. S. (eds), *Evolution of African Mammals*. Harvard University Press, Cambridge, Massachusetts: 509-535. https://doi.org/10.4159/harvard.9780674431263.c26
Danowitz M., Vasilyev A., Kortlandt V. & Solounias N. 2015. — Fossil evidence and stages of elongation of the *Giraffa camelopardalis* neck. *Royal Society Open Science* 2: 150393. https://doi.org/10.1098/rsos.150393
De Vos J., Van Der Made J., Athanassiou A., Lyras G., Sondaar P. & Dermitzakis M. D. 2002. — Preliminary note on the Late Pliocene fauna from Vatera (Lesvos, Greece). *Annales géologiques des Pays helléniques*, série 39, A: 37-70.
Gaudry A. 1861. — Note sur la girafe et l'*Helladotherium* trouvées à Pikermi (Grèce). *Bulletin de la Societé géologique de France* 2ème série, 5: 587-597.
Gentry A. W. 2003. — Ruminantia (Artiodactyla), *in* Fortelius M., Kappelman J., Sen S. & Bernor R. L. (eds), *Geology and Paleontology of the Miocene Sinap Formation, Turkey*. Columbia University Press, New York: 332-379.
Gentry A. W., Rössner G. E. & Heizmann E. P. J. 1999. — Suborder Ruminantia, *in* Rössner G. E. & Heissig K. (eds), *The Miocene Land Mammals of Europe*. Verlag Dr. Friedrich Pfeil, Munich: 225-258.
Geraads D. 1974. — *Les Giraffidés du Miocène supérieur de la région de Thessalonique (Grèce)*. PhD thesis, University of Paris VI, 87 p.
Geraads D. 1978. — Les Palaeotraginae (Giraffidae, Mammalia) du Miocène supérieur de la région de Thessalonique (Grèce). *Géologie méditerranéenne* 5 (2): 269-276. https://doi.org/10.3406/geolm.1978.1048
Geraads D. 1979. — Les Giraffinae (Artiodactyla, Mammalia) du Miocène supérieur de la région de Thessalonique (Grèce). *Bulletin du Muséum national d'Histoire naturelle*, 4ème série, *Section C, Sciences de la Terre, Paléontologie, Géologie, Minéralogie* 1 (4): 377-389. https://www.biodiversitylibrary.org/page/55602823
Geraads D. 1986. — Remarques sur la systématique et la phylogénie des Giraffidae (Artiodactyla, Mammalia). *Geobios* 19 (4): 465-477. https://doi.org/10.1016/S0016-6995(86)80004-3

GERAADS D. 1994. — Les gisements de mammifères du Miocène supérieur de Kemiklitepe, Turquie : 8. Giraffidae. *Bulletin du Muséum national d'Histoire naturelle*, 4ème série, *Section C, Sciences de la Terre, Paléontologie, Géologie, Minéralogie* 16 (1): 159-173. https://www.biodiversitylibrary.org/page/55872554

GERAADS D. 2013. — Large Mammals from the Late Miocene of Çorakyerler, Çankırı, Turkey. *Acta Zoologica Bulgarica* 65 (3): 381-390.

GERAADS D., REED K. & BOBE R. 2013. — Pliocene Giraffidae (Mammalia) from the Hadar Formation of Hadar and Ledi-Geraru, Lower Awash, Ethiopia. *Journal of Vertebrate Paleontology* 32 (2): 470-481. https://doi.org/10.1080/02724634.2013.723657

GODINA A. Y. 1975. — [*Palaeotragus* from the Neogene deposits of Western Mongolia and Central Asia], *in* Iskopaemaya fauna i flora Mongolii (Fossil Fauna and Flora of Mongolia). *Transactions of United Soviet-Mongolian Palaeontology Expedition,* volume 2: 67-75 (in Russian).

GODINA A. Y. 1979. — [*History of Fossil Giraffes of the Genus* Palaeotragus]. Trudy, Paleontological Institut Akademia Nauk SSSR, 177: 1-114, Moscow (in Russian).

GODINA A. Y. 2002. — On the taxonomy and evolution of *Samotherium* (Giraffidae, Artiodactyla). *Paleontological Journal* 36 (4): 395-402.

GRAY J. E. 1821. — On the natural arrangement of vertebrate animals. *London Medical Repository* 15: 296-310.

HAMILTON W. R. 1978. — Fossil giraffes from the Miocene of Africa and a revision of the phylogeny of the Giraffoidea. *Philosophical Transactions of the Royal Society of London B: Biological Sciences* 283 (996): 165-229. https://doi.org/10.1098/rstb.1978.0019

HAMMER Ø., HARPER D. A. T. & RYAN P. D. 2001. — PAST: Palaeontological statistics software package for education and data analysis. *Palaeontologia Electronica* 4: 1-9.

HOU S., DANOWTIZ M., SAMMIS J. & SOLOUNIAS N. 2014. — Dead ossicones and other characters describing Palaeotragiinae (Giraffidae; Mammalia) based on new material from Gansu, Central China. *Zitteliana* B 32 (91): 91-98. https://doi.org/10.5282/ubm/epub.22389

ILIOPOULOS G. 2003 (published 2015). — *The Giraffidae (Mammalia, Artiodactyla) and the Study of the Histology and Chemistry of Fossil Mammal Bone from the Late Miocene of Kerassia (Euboea Island, Greece)*. PhD thesis, Geology Department, University of Leicester; ProQuest LLC, UMI195587, Ann Arbor, 144 p. https://hdl.handle.net/2381/35044

KOKEN E. 1885. — Über fossile Säugethiere aus China. *Palaeontologische Abhandlungen* 3: 31-113.

KONIDARIS G. E. 2013. — *Palaeontological and Biostratigraphical of the Neogene Proboscidea from Greece.* PhD thesis, Aristotle University of Thessaloniki, 326 p. (in Greek with English summary).

KOROTKEVICH E. L. 1957. — Giraffes in *Hipparion* fauna of Berislav. *Trudy Zoological Institute Academia Nauk USSR* 14: 129-140 (in Ukranian with Russian abstract).

KOSTOPOULOS D. S. 2009. — 13. Giraffidae, *in* KOUFOS G.D. & NAGEL D. (eds), The Late Miocene Mammal Faunas of Samos Island, Greece: new collection. *Beiträge zur Paläontologie* 31: 299-343.

KOSTOPOULOS D. S & KOUFOS G. D. 1994. — The Plio-Pleistocene artiodactyls of Macedonia (Northern Greece) and their biostratigraphic significance; preliminary report. *Comptes rendus de l'Académie des Sciences, série 2A, Sciences de la Terre et des Planètes* 318 (9): 1267-1272. https://gallica.bnf.fr/ark:/12148/bpt6k62102902/f73.item

KOSTOPOULOS D. S., KOLIADIMOU K. K. & KOUFOS G. D. 1996. — The giraffids (Mammalia, Artiodactyla) from the Late Miocene mammalian localities of Nikiti (Macedonia, Greece). *Palaeontographica Abteilung A* 239 (1-3): 61-88. https://doi.org/10.1127/pala/239/1996/61

KOSTOPOULOS D. S. & SARAÇ G. 2005. — Giraffidae (Mammalia, Artiodactyla) from the Late Miocene of Akkaşdağı, Turkey, *in* SEN S. (ed.), Geology, Mammals and Environments at Akkaşdağı, Late Miocene of Central Anatolia. *Geodiversitas* 27: 735-745.

KOSTOPOULOS D. S. & KOUFOS G. D. 2006. — The Late Miocene vertebrate locality of Perivolaki, Thessaly, Greece: 8. Giraffidae. *Palaeontographica Abteilung A,* 276 (1-6): 135-149.

KOUFOS G. D. 1990. — The hipparions of the Lower Axios valley (Macedonia, Greece). Implications about the Neogene biostratigraphy and the evolution of the *Hipparion, in* LINDSAY E.H., FAHLBUSH V. & MEIN P. (eds), *European Neogene Mammal Chronology.* Plenum Press, the NATO ASI book series (NSSA, volume 180), New York: 321-328. https://doi.org/10.1007/978-1-4899-2513-8_19

KOUFOS G. D. 2006. — The Neogene mammal localities of Greece: Faunas, chronology and biostratigraphy. *Hellenic Journal of Geosciences* 41:183-214.

KOUFOS G. D. 2016. — History, stratigraphy and fossiliferous sites, *in* KOUFOS G. D. & KOSTOPOULOS D. S. (eds), Palaeontology of the upper Miocene vertebrate localities of Nikiti (Chalkidiki Peninsula, Macedonia, Greece). *Geobios* 49 (1-2): 3-10. https://doi.org/10.1016/j.geobios.2016.01.007

KOUFOS G. D., SYRIDES G. KOLIADIMOU K. K. & KOSTOPOULOS D. S. 1991. — Un nouveau gisement de vertébrés avec hominoïde dans le Miocène supérieur de Macédoine (Grèce). *Comptes rendus de l'Académie des Sciences. Série 2, Mécanique, Physique, Chimie, Sciences de l'Univers, Sciences de la Terre* 313: 691-696. https://gallica.bnf.fr/ark:/12148/bpt6k54893445/f691.item

KOUFOS G. D., KOSTOPOULOS D. S., VLACHOU T. D. & KONIDARIS G. E. 2016. — Revision of the Nikiti 1 (NKT) fauna with description of new material. *Geobios* 49 (1-2): 11-22. https://doi.org/10.1016/j.geobios.2016.01.006

LAZARIDIS G. 2015. — *Study of the Late Miocene Vertebrate Locality of Kryopigi and other Localities of Kasssandra Peninsula, Chalkidiki (Greece). Systematics, Taphonomy, Paleoecology, Biochronology*. PhD thesis, School of Geology, Aristotle university of Thessaloniki Scientific Annals of the School of Geology, Aristotle University, Thessaloniki, Greece, 376 p. (in Greek with English summary).

OWEN R. 1848. — *On the Archetype and Homologies of the Vertebrate Skeleton*. Richard and John E. Taylor, London, 203 p. https://doi.org/10.5962/bhl.title.118611

OZANSOY F. 1965. — Études des gisements continentaux et des mammifères du Cénozoïque de Turquie. *Mémoires de la Societé géologique de France, N.S.,* 44 (1): 1-92.

PAVLOW M. 1913. — Mammifères tertiaires de la Nouvelle Russie. *Nouveaux mémoires de la Société impériale des Naturalistes de Moscou* 17 (3): 1-67. https://www.biodiversitylibrary.org/page/54280248

PILGRIM G.E. 1911. — The Fossil Giraffidae of India. *Memoirs of the Geological Survey of India* 4: 1-29.

RÍOS M., DANOWITZ M. & SOLOUNIAS N. 2016. — First comprehensive morphological analysis on the metapodials of Giraffidae. *Palaeontologia Electronica* 19.3.50A: 1-39. https://doi.org/10.26879/653

RÍOS M., SANCHEZ I. M. & MORALES J. 2017 — A new giraffid (Mammalia, Ruminantia, Pecora) from the late Miocene of Spain, and the evolution of the sivathere-samothere lineage. *PLoS ONE* 12 (11): e0185378. https://doi.org/10.1371/journal.pone.0185378

RODLER A. & WEITHOFER K. A. 1890. — Die Wiederkäuer der Fauna von Maragha. *Denkschriften der Kaiserlichen Akademie der Wissenschaften Wien* 57: 753-772. https://www.biodiversitylibrary.org/page/7129582

SEN S., KOUFOS G. D, KONDOPOULOU D., & DE BONIS L. 2000. — Magnetostratigraphy of the late Miocene continental deposits of the lower Axios valley, Macedonia, Greece, *in* KOUFOS G. D. & IOAKIM C. E. (eds), Mediterranean Neogene cyclostratigraphy in marine-continental palaeoenvironments. *Geological Society of Greece Special Publications* 9: 197-206.

SCHMID E. 1972. — *Atlas of Animal Bones for Prehistorians, Archaeologists and Quaternary Geologists.* Elsevier Publishing Company, Amsterdam, 167 p.

SOLOUNIAS N. & DANOWITZ M. 2016. — Astragalar Morphology of Selected Giraffidae. *PLoS ONE* 11(3): e0151310. https://doi.org/10.1371/journal.pone.0151310

Steensma K. J. 1988. — *Plio-/Pleistozäne Großsäugetiere (Mammalia) aus dem Becken von Kastoria / Grevena, südlich von Neapolis – NW Griechenland*. PhD thesis, Technische Universität Clausthal, 315 p.

Von Der Driesch A. 1976. — *A Guide to the Measurement of Animal Bones from Archaeological Sites.* Peabody Museum Bulletins, Harvard University, Cambridge, 148 p.

Xafis A., Tsoukala E., Solounias N., Mandic O., Harzhauser M., Grímsson F. & Nagel D. 2019. — Fossil Giraffidae (Mammalia, Artiodactyla) from the Late Miocene of Thermopigi (Macedonia, Greece). *Palaeontologia Electronica* 22 (3.68): 1-38. https://doi.org/10.26879/889

*Submitted on 10 November 2020;*
*accepted on 6 January 2021;*
*published on 14 April 2022.*

# APPENDICES

APPENDIX 1. — Biometrical variables and selected premolar features of Late Miocene Eurasian palaeotrages used in multivariate analyses (Fig. 11 main text; Appendix 3: Figs S1, S2).

| | |
|---|---|
| Lpm | Lower toothrow length; |
| Lp | Lower premolar row length; |
| Lm | Lower molar row length; |
| | ×100 (p/pm); |
| | ×100 (p/m); |
| | ×100 (m/pm); |
| LPM | Upper toothrow length; |
| LP | Upper premolar row length; |
| LM | Upper molar row length; |
| | ×100 (P/PM) |
| | ×100 (P/M) |
| | ×100 (M/PM) |
| R-GL | Greatest length of the radii; |
| R-Bp | Breadth of the radii proximal end; |
| Mc-GL | Greatest length of the metacarpals; |
| Mc-Bdia | Breadth of the metacarpals' diaphysis; |
| Mc-R.I. | Metacarpals' robusticity index (×100); |
| T-Bd | Breadth of the tibiae distal end; |
| T-Dd | Depth of the tibiae distal end; |
| A-GLl | Greatest lateral length of the astragali; |
| A-Bd | Breadth of the astragali distal end; |
| Mt-GL | Greatest length of the metatarsals |
| Mt-Bdia | Breadth of the metatarsals' diaphysis; |
| Mt-Ddia | Depth of the metatarsals' diaphysis; |
| Mt-R.I. | Metatarsals R.I.; |
| Mt-Bp | Breadth of the metatarsals proximal end; |
| Mt-Dp | Depth of the metatarsals proximal end; |

$P_3$ morphology

| | |
|---|---|
| 0 | primitive ruminant morphology; |
| 1 | molarized. |

$P^4$ lingual groove

| | |
|---|---|
| 0 | absent; |
| 1 | present. |

$P^4$ lingual stylids

| | |
|---|---|
| 0 | absent; |
| 1 | present. |

$P^4$ occusal shape

| | |
|---|---|
| 0 | circular; |
| 1 | triangular; |
| 2 | squared. |

APPENDIX 2. — Tables 1-14: Measurements of *Palaeotragus coelophrys* (Rodler & Weithofer, 1890).

TABLE 1. — Measurements of *Palaeotragus coelophrys* upper teeth from Pentalophos (PNT). Abbreviations: **LPM**, Length of upper toothrow; **LP**, Length of upper premolar row; **LM**, Length of upper molar row; **$LP^2$**, Length of $P^2$; **$WP^2$**, Width of $P^2$; **$LP^3$**, Length of $P^3$; **$WP^3$**, Width of $P^3$; **$LP^4$**, Length of $P^4$; **$WP^4$**, Width of $P^4$; **$LM^1$**, Length of $M^1$; **$WaM^1$**, Width of $M^1$ anterior lobe; **$WpM^1$**, Width of $M^1$ posterior lobe; **$LM^2$**, Length of $M^2$; **$WaM^2$**, Width of $M^2$ anterior lobe; **$WpM^2$**, Width of $M^2$ posterior lobe; **$LM^3$**, Length of $M^3$; **$WaM^3$**, Width of $M^3$ anterior lobe; **$WpM^3$**, Width of $M^3$ posterior lobe (in mm).

| | Specimen Reg. no. PNT- | | | | | |
|---|---|---|---|---|---|---|
| **Measurements** | **113** | **165** | **152** | **163** | **161** | **164** |
| LPM | 138.45 | – | – | – | – | – |
| LP | 59.5 | – | – | – | – | – |
| LM | 82.14 | – | – | – | – | – |
| $LP^2$ | 17.42 | – | 20.06 | 19.32 | 19.02 | – |
| $WP^2$ | 19.54 | – | 18.73 | 19.54 | 19.17 | – |
| $LP^3$ | 20.21 | – | 20.53 | 20.8 | – | 21.4 |
| $WP^3$ | 21.2 | – | 21.65 | 24.37 | – | 24.1 |
| $LP^4$ | 20.47 | – | – | – | – | – |
| $WP^4$ | 26.05 | – | – | – | – | – |
| $LM^1$ | 26.8 | – | – | – | – | – |
| $WaM^1$ | 28.13 | – | – | – | – | – |
| $WpM^1$ | 27.62 | – | – | – | – | – |
| $LM^2$ | 30.1 | 28.6 | – | – | – | – |
| $WaM^2$ | 31.06 | 28.15 | – | – | – | – |
| $WpM^2$ | 26.8 | 26.23 | – | – | – | – |
| $LM^3$ | 29.36 | 31.64 | – | – | – | – |
| $WaM^3$ | 18.1 | 30.26 | – | – | – | – |
| $WpM^3$ | 24.18 | 26.74 | – | – | – | – |

TABLE 2. — Measurements of *Palaeotragus coelophrys* lower teeth from Pentalophos (PNT). Abbreviations: **LM**, Length of lower molar row; **$LP_2$**, Length of $P_2$; **$WP_2$**, Width of $P^2$; **$LP_3$**, Length of $P_3$; **$WP_3$**, Width of $P_3$; **$LP_4$**, Length of $P_4$; **$WP_4$**, Width of $P_4$; **$LM_1$**, Length of $M_1$; **$WaM_1$**, Width of $M_1$ anterior lobe; **$WpM_1$**, Width of $M_1$ posterior lobe; **$LM_2$**, Length of $M_2$; **$WaM_2$**, Width of $M_2$ anterior lobe; **$WpM_2$**, Width of $M_2$ posterior lobe; **$LM_3$**, Length of $M_3$; **$WaM_3$**, Width of $M_3$ anterior lobe; **$WpM_3$**, Width of $M_3$ posterior lobe (in mm).

| **Measurements** | **Specimen Reg. no. PNT-328F** |
|---|---|
| LM | 97 |
| $LM_1$ | 28.18 |
| $WaM_1$ | 18.55 |
| $WpM_1$ | 21.45 |
| $LM_2$ | 28.05 |
| $WaM_2$ | 22.31 |
| $WpM_2$ | 23.5 |
| $LM_3$ | 38.08 |
| $WaM_3$ | 21.37 |
| $WpM_3$ | 21.96 |
| $W3M_3$ | 16.7 |

TABLE 3. — Measurements of *Palaeotragus coelophrys* lower deciduous teeth from Pentalophos (PNT). Abbreviations: **LdP**, Length of deciduous lower premolar row; **$LdP_2$**, Length of $dP_2$; **$WdP_2$**, Width of $dP^2$; **$LdP_3$**, Length of $dP_3$; **$WdP_3$**, Width of $dP_3$; **$LdP_4$**, Length of $dP_4$; **$WdP_4$**, Width of $dP_4$; **$LM_1$**, Length of $M_1$; **$WaM_1$**, Width of $M_1$ anterior lobe; **$WpM_1$**, Width of $M_1$ posterior lobe (in mm).

| Measurements | Specimen Reg. no. PNT-121F |
|---|---|
| LdP | 69.79 |
| $LdP_2$ | 15.82 |
| $WdP_2$ | 8.38 |
| $LdP_3$ | 22.98 |
| $WdP_3$ | 9.71 |
| $LdP_4$ | 31.03 |
| $WadP_4$ | 11.34 |
| $WmdP_4$ | 16.23 |
| $Wpdp_4$ | 16.14 |
| $LM_1$ | 28.88 |
| $WaM_1$ | 20.12 |
| $WpM_1$ | 20.06 |

TABLE 4. — Measurements of *Palaeotragus coelophrys* metatarsals from Pentalophos (PNT). Abbreviations: **Mt-Bp**, Breadth of metatarsal proximal end; **Mt-Dp**, Depth of metatarsal proximal end; **Mt-Bdia**, Breadth of metatarsal at the middle of the shaft; **Mt-Ddia**, Depth of metatarsal at the middle of the shaft (in mm).

| | Specimen Reg. no. | |
|---|---|---|
| Measurements | PNT-119F | PNT-114F |
| Mt-Bp | 62.98 | 60.39 |
| Mt-Dp | 60.75 | 57.58 |
| Mt-Bdia | 37.02 | 40.66 |
| Mt-Ddia | 37.20 | 32.81 |

TABLE 5. — Measurements of *Palaeotragus* cf. *coelophrys* upper teeth from the Ravin de la Pluie (cranium RPI-91B). Abbreviations: **LPM**, Length of upper toothrow; **LP**, Length of upper premolar row; **LM**, Length of upper molar row; **$LP^2$**, Length of $P^2$; **$WP^2$**, Width of $P^2$; **$LP^3$**, Length of $P^3$; **$WP^3$**, Width of $P^3$; **$LP^4$**, Length of $P^4$; **$WP^4$**, Width of $P^4$; **$LM^1$**, Length of $M^1$; **$WaM^1$**, Width of $M^1$ anterior lobe; **$WpM^1$**, Width of $M^1$ posterior lobe; **$LM^2$**, Length of $M^2$; **$WaM^2$**, Width of $M^2$ anterior lobe; **$WpM^2$**, Width of $M^2$ posterior lobe; **$LM^3$**, Length of $M^3$; **$WaM^3$**, Width of $M^3$ anterior lobe; **$WpM^3$**, Width of $M^3$ posterior lobe (in mm).

| | Specimen Reg. no. | |
|---|---|---|
| Measurements | RPI-91B left | RPI-91B right |
| LPM | 152.25 | 147.4 |
| LP | 68.68 | 62.81 |
| LM | 94.07 | 85.41 |
| $LP^2$ | 18.82 | 22.88 |
| $WP^2$ | 20.44 | 20.62 |
| $LP^3$ | 21.61 | 21.25 |
| $WP^3$ | 23.67 | 22.61 |
| $LP^4$ | 21.14 | 19.21 |
| $WP^4$ | 26.04 | 26.64 |
| $LM^1$ | 24.82 | 23.96 |
| $WaM^1$ | 26.85 | 27.42 |
| $WpM^1$ | 26.28 | 26.85 |
| $LM^2$ | 28.50 | 30.51 |
| $WaM^2$ | 29.21 | 28.70 |
| $WpM^2$ | 27.81 | 27.38 |
| $LM^3$ | 28.63 | 28.47 |
| $WaM^3$ | 28.18 | 26.41 |
| $WpM^3$ | 24.59 | 22.41 |

TABLE 6. — Measurements of *Palaeotragus* cf. *coelophrys* lower teeth from Ravin de la Pluie (RPI). Abbreviations: **LM**, Length of lower molar row; **$LP_2$**, Length of $P_2$; **$WP_2$**, Width of $P^2$; **$LP_3$**, Length of $P_3$; **$WP_3$**, Width of $P_3$; **$LP_4$**, Length of $P_4$; **$WP_4$**, Width of $P_4$; **$LM_1$**, Length of $M_1$; **$WaM_1$**, Width of $M_1$ anterior lobe; **$WpM_1$**, Width of $M_1$ posterior lobe; **$LM_2$**, Length of $M_2$; **$WaM_2$**, Width of $M_2$ anterior lobe; **$WpM_2$**, Width of $M_2$ posterior lobe; **$LM_3$**, Length of $M_3$; **$WaM_3$**, Width of $M_3$ anterior lobe; **$WpM_3$**, Width of $M_3$ posterior lobe (in mm).

| Measurements | Specimen Reg. no. RPI-104 |
|---|---|
| LM | 89.59 |
| $LM_1$ | 24.92 |
| $WaM_1$ | 17.09 |
| $WpM_1$ | 17.38 |
| $LM_2$ | 25.80 |
| $WaM_2$ | 18.30 |
| $WpM_2$ | 19.24 |
| $LM_3$ | 39.15 |
| $WaM_3$ | 18.89 |
| $WpM_3$ | 19.91 |
| $W3M_3$ | 10.97 |

TABLE 7. — Measurements of *Palaeotragus* sp. lower teeth from Xirochori (XIR). **$LM_2$**, Length of $M_2$; **$WaM_2$**, Width of $M_2$ anterior lobe; **$WpM_2$**, Width of $M_2$ posterior lobe; **$LM_3$**, Length of $M_3$; **$WaM_3$**, Width of $M_3$ anterior lobe; **$WpM_3$**, Width of $M_3$ posterior lobe (in mm).

| Measurements | Specimen Reg. no. XIR-24 |
|---|---|
| $LM_2$ | 26.93 |
| $WaM_2$ | 19.55 |
| $WpM_3$ | 19.04 |
| $LM_3$ | 40.33 |
| $WaM_3$ | 20.06 |
| $WpM_3$ | 20.00 |
| $W3M_3$ | 11.95 |

TABLE 8. — Measurements of *Palaeotragus* aff. *berislavicus* upper teeth from the Nikiti (cranium NKT-172). Abbreviations: **LPM**, Length of upper toothrow; **LP**, Length of upper premolar row; **LM**, Length of upper molar row; **$LP^2$**, Length of $P^2$; **$WP^2$**, Width of $P^2$; **$LP^3$**, Length of $P^3$; **$WP^3$**, Width of $P^3$; **$LP^4$**, Length of $P^4$; **$WP^4$**, Width of $P^4$; **$LM^1$**, Length of $M^1$; **$WaM^1$**, Width of $M^1$ anterior lobe; **$WpM^1$**, Width of $M^1$ posterior lobe; **$LM^2$**, Length of $M^2$; **$WaM^2$**, Width of $M^2$ anterior lobe; **$WpM^2$**, Width of $M^2$ posterior lobe; **$LM^3$**, Length of $M^3$; **$WaM^3$**, Width of $M^3$ anterior lobe; **$WpM^3$**, Width of $M^3$ posterior lobe (in mm).

| | Specimen Reg. no. | |
|---|---|---|
| Measurements | NKT-172 left | NKT-172 right |
| LPM | 141.41 | 146.1 |
| LP | 62.35 | 63.49 |
| LM | 85.10 | 84.9 |
| $LP^2$ | 22.40 | 21.61 |
| $WP^2$ | 18.93 | 18.91 |
| $LP^3$ | 20.79 | 21.20 |
| $WP^3$ | 23.5 | 21.18 |
| $LP^4$ | 20.66 | 20.14 |
| $WP^4$ | 27.26 | 24.72 |
| $LM^1$ | 25.59 | 29.46 |
| $WaM^1$ | – | 27.80 |
| $WpM^1$ | – | 26.30 |
| $LM^2$ | 29.87 | 30.22 |
| $WaM^2$ | 33.29 | 28.14 |
| $WpM^2$ | – | 28.25 |
| $LM^3$ | 27.66 | 30.58 |
| $WaM^3$ | 141.41 | 31.63 |
| $WpM^3$ | 62.35 | 27.68 |

TABLE 9. — Measurements of *Palaeotragus* aff. *berislavicus* radii from Nikiti (NKT). **R-GL**, Greatest Length; **R-Bp**, Breadth of the proximal end; **R-Dp**, Depth of the proximal end; **R-Bpart**, Breadth of the proximal articular surface; **R-Bdia**, Breadth in the middle of the shaft; **R-Ddia**, Depth In the middle of the shaft; **R-Bd**, Breadth of the distal end; **R-Dd**, Depth of the distal end (in mm).

| | Specimen Reg. no. | | | | |
|---|---|---|---|---|---|
| **Measurements** | **NKT-159** | **NKT-167** | **NKT-156** | **NKT-155** | **NKT-169** |
| R-GL | 449 | – | 462 | 476 | 470 |
| R-Bp | 82.42 | 88.05 | 81.24 | 82.82 | 71.45 |
| R-Dp | 53.25 | 46.82 | 44.64 | 49.00 | 40.74 |
| R-Bpart | – | – | 67.95 | 73.83 | – |
| R-Bdia | 48.18 | 48.25 | 51.47 | 49.61 | 51.25 |
| R-Ddia | 36.03 | 35.02 | 41.64 | 33.26 | 30.77 |
| R-Bd | 75.51 | – | 75.66 | 80.59 | 73.95 |
| R-Dd | 55.17 | – | 54.47 | 51.78 | 42.60 |

TABLE 10. — Measurements of *Palaeotragus* aff. *berislavicus* metacarpals from Nikiti (NKT). **Mc-GL**, Greatest Length; **Mc-Bp**, Breadth of the proximal end; **Mc-Dp**, Depth of the proximal end; **Mc-Bdia**, Breadth in the middle of the shaft; **Mc-Ddia**, Depth In the middle of the shaft; **Mc-Bd**, Breadth of the distal end; **Mc-Dd**, Depth of the distal end (in mm).

| | Specimen Reg. no. | | | | |
|---|---|---|---|---|---|
| **Measurements** | **NKT-141** | **NKT-137** | **NKT-131** | **NKT-67** | **NKT-26** |
| Mc-GL | 409.0 | 378.0 | 380.0 | – | – |
| Mc-Bp | 64.68 | 57.89 | 64.60 | 70.37 | 61.15 |
| Mc-Dp | 40.25 | 32.71 | 46.55 | 39.63 | 41.28 |
| Mc-Bdia | 35.80 | 31.68 | 32.79 | 42.30 | – |
| Mc-Ddia | 31.44 | 31.21 | 30.74 | 30.79 | – |
| Mc-Bd | 63.41 | 60.26 | 61.65 | – | – |
| Mc-Dd | 38.19 | 35.56 | 37.16 | – | – |

TABLE 11. — Measurements of *Palaeotragus* aff. *berislavicus* tibiae from Nikiti (NKT). **T-GL**, Greatest Length; **T-Bp**, Breadth of the proximal end; **T-Dp**, Depth of the proximal end; **T-Bdia**, Breadth in the middle of the shaft; **T-Ddia**, Depth In the middle of the shaft; **T-Bd**, Breadth of the distal end; **T-Dd**, Depth of the distal end (in mm).

| | Specimen Reg. no. | | |
|---|---|---|---|
| **Measurements** | **NKT-271** | **NKT-150** | **NKT-154** |
| T-GL | 451.0 | – | – |
| T-Bp | 82.57 | – | – |
| T-Dp | 82.07 | – | – |
| T-Bdia | 50.40 | 45.49 | 47.78 |
| T-Ddia | 35.53 | 36.98 | 39.60 |
| T-Bd | 81.60 | 67.53 | 68.90 |
| T-Dd | 55.79 | 54.73 | 45.77 |

TABLE 12. — Measurements of *Palaeotragus* aff. *berislavicus* astragali from Nikiti (NKT). **A-GLl**, Greatest lateral Length; **A-GLm**, Greatest medial Length; **A-Bp**, Breadth of the proximal end; **A-Dl**, Lateral Depth; **A-Dm**, Medial Depth; **A-Bd**, Breadth of the distal end (in mm).

| | Specimen Reg. no. | | |
|---|---|---|---|
| **Measurements** | **NKT-267** | **NKT-163** | **NKT-266** |
| A-GLl | 78.58 | 77.83 | 78.64 |
| A-GLm | 70.75 | 72.57 | 67.41 |
| A-Bp | 49.29 | 52.01 | 50.17 |
| A-Dl | 45.40 | 43.42 | 49.20 |
| A-Dm | 47.25 | 46.36 | 51.30 |
| A-Bd | 47.03 | 50.96 | 50.00 |

TABLE 13. — Measurements of *Palaeotragus* aff. *berislavicus* calcanei from Nikiti (NKT). **C-GLl**, Greatest Length; **C-GB**, Greatest Breadth (in mm).

| | Specimen Reg. no. | |
|---|---|---|
| **Measurements** | **NKT-268** | **NKT-153** |
| C-GL | 136.61 | 147.35 |
| C-GB | 45.76 | 55.00 |

TABLE 14. — Measurements of *Palaeotragus* aff. *berislavicus* metatarsals from Nikiti (NKT). **Mt-GL**, Greatest Length; **Mt-Bp**, Breadth of the proximal end; **Mt-Dp**, Depth of the proximal end; **Mt-Bdia**, Breadth in the middle of the shaft; **Mt-Ddia**, Depth In the middle of the shaft; **Mt-Bd**, Breadth of the distal end; **Mt-Dd**, Depth of the distal end (in mm).

| | Specimen Reg. no. | | | | | | | | | |
|---|---|---|---|---|---|---|---|---|---|---|
| **Measurements** | **NKT-136** | **NKT-160** | **NKT-139** | **NKT-133** | **NKT-144** | **NKT-138** | **NKT-168** | **NKT-151** | **NKT-140** | **NKT-132** |
| Mt-GL | 414 | 409 | 386 | 412 | 415 | 436 | – | – | – | – |
| Mt-Bp | 58.86 | 60.85 | 52.45 | 62.76 | 59.50 | 59.46 | 56.44 | – | 58.42 | 54.81 |
| Mt-Dp | 57.83 | 49.49 | 54.62 | 53.06 | 45.71 | – | 50.44 | – | 44.82 | – |
| Mt-Bdia | 34.22 | 41.25 | 33.65 | 49.60 | 33.35 | 31.94 | 38.48 | 40.73 | 40.98 | 32.80 |
| Mt-Ddia | 33.58 | 34.93 | 29.68 | 28.75 | 33.05 | 30.21 | 36.30 | 31.35 | 34.00 | 35.18 |
| Mt-Bd | – | 64.80 | 57.84 | 60.56 | 57.89 | – | – | 61.19 | – | – |
| Mt-Dd | – | 38.49 | 35.30 | 40.47 | 35.68 | 33.92 | – | 37.81 | – | – |

Appendix 3. — Figures S1 à S12.

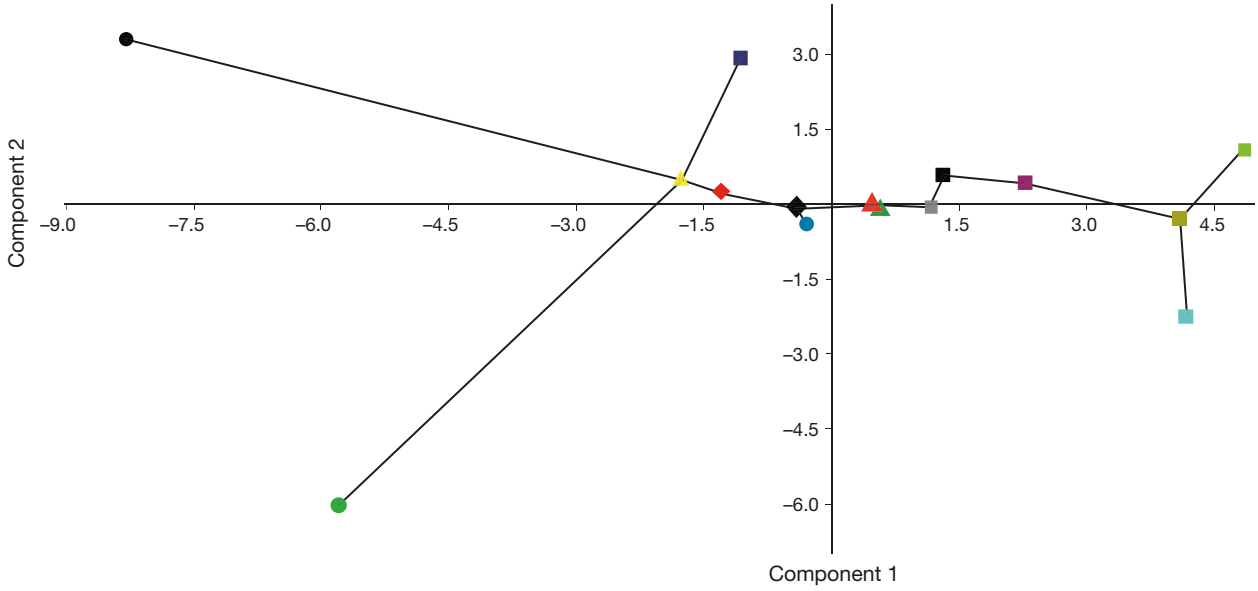


Fig. S1. — Principal Components Analysis (plane of components 1 and 2, representing 40,3% and 14,4% respectively of initial data variance) comparing 27 biometrical variables and 4 selected features of premolar morphology of the Late Miocene Eurasian palaeotrages as well as the Vallesian Greek samples studied here.


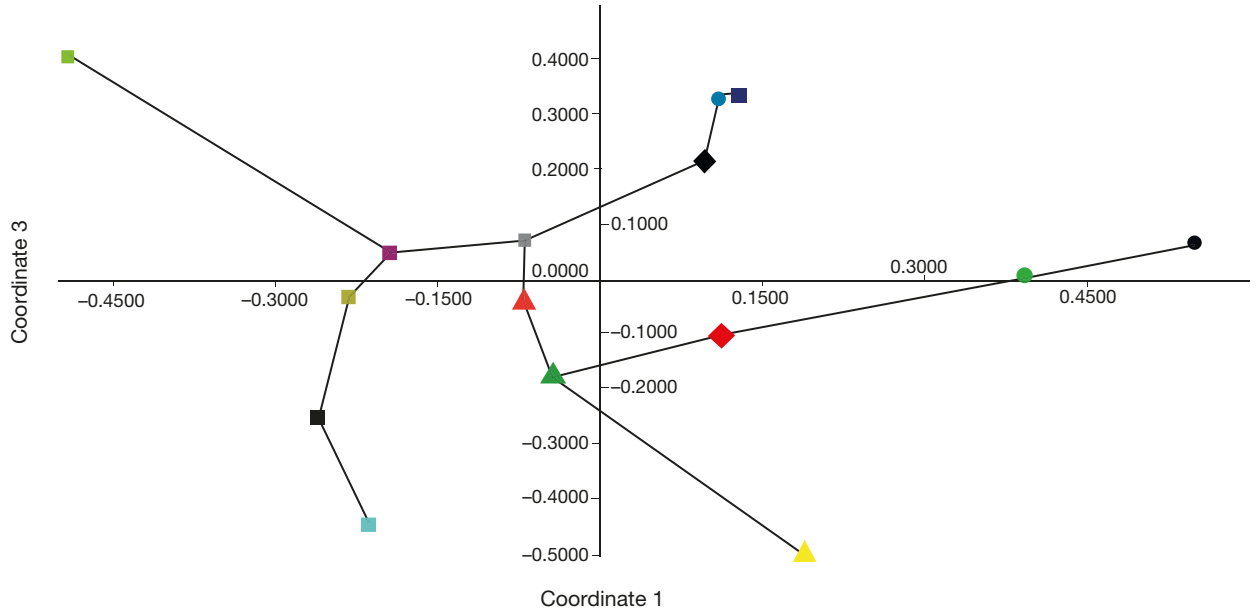


Fig. S2. — Principal Coordinates Analysis (plane of coordinates 1 and 3, representing 39,5% and 10,4% respectively of initial data variance) comparing 27 biometrical variables and 4 selected features of premolar morphology of the Late Miocene Eurasian palaeotrages as well as the Vallesian Greek samples studied here.

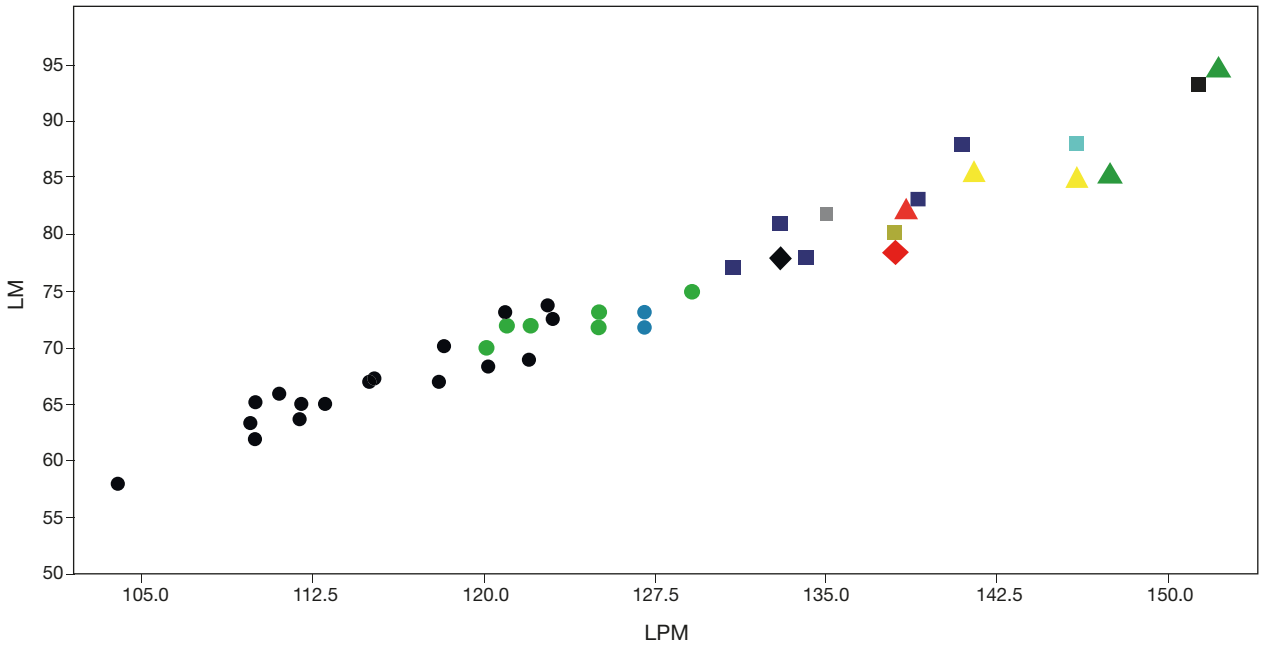


FIG. S3. — Scatter plot of upper teeth proportions of the Late Miocene Eurasian palaeotrages as well as the Vallesian Greek samples studied here. Abbreviations: **LM**, length of molar row; **LPM**, length of toothrow.


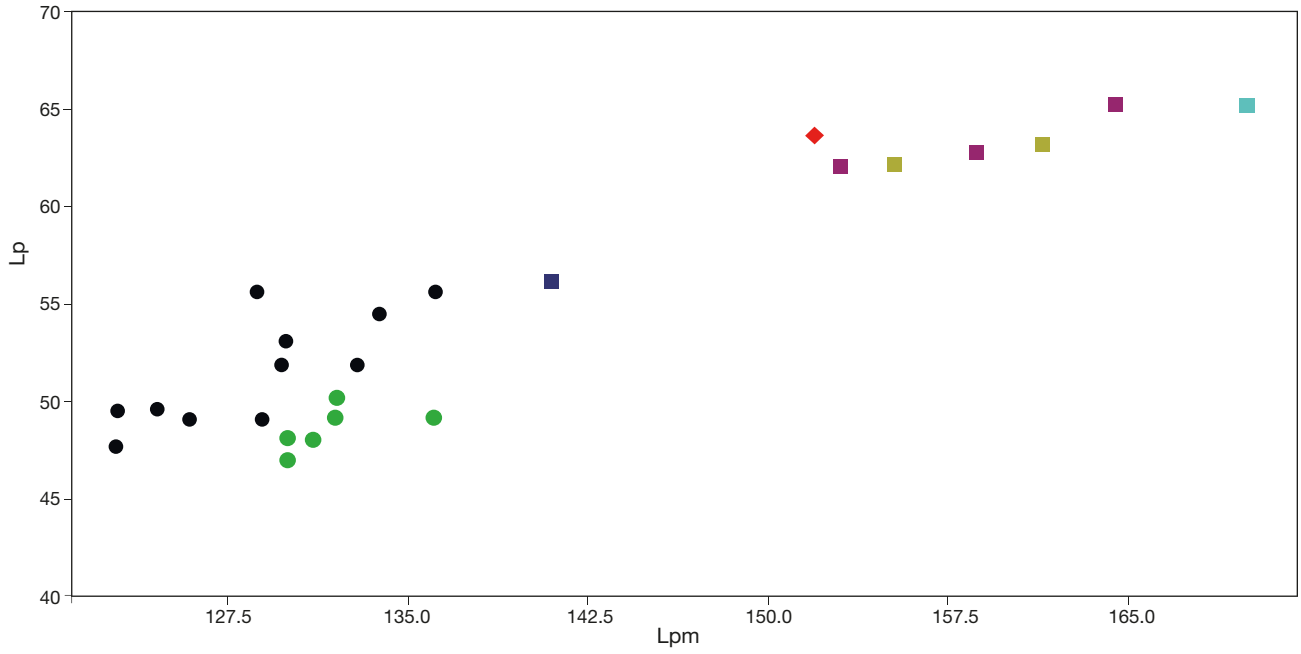


FIG. S4. — Scatter plot of lower teeth proportions of the Late Miocene Eurasian palaeotrages. Abbreviations: **Lp**, length of premolar row; **Lpm**, length of toothrow.

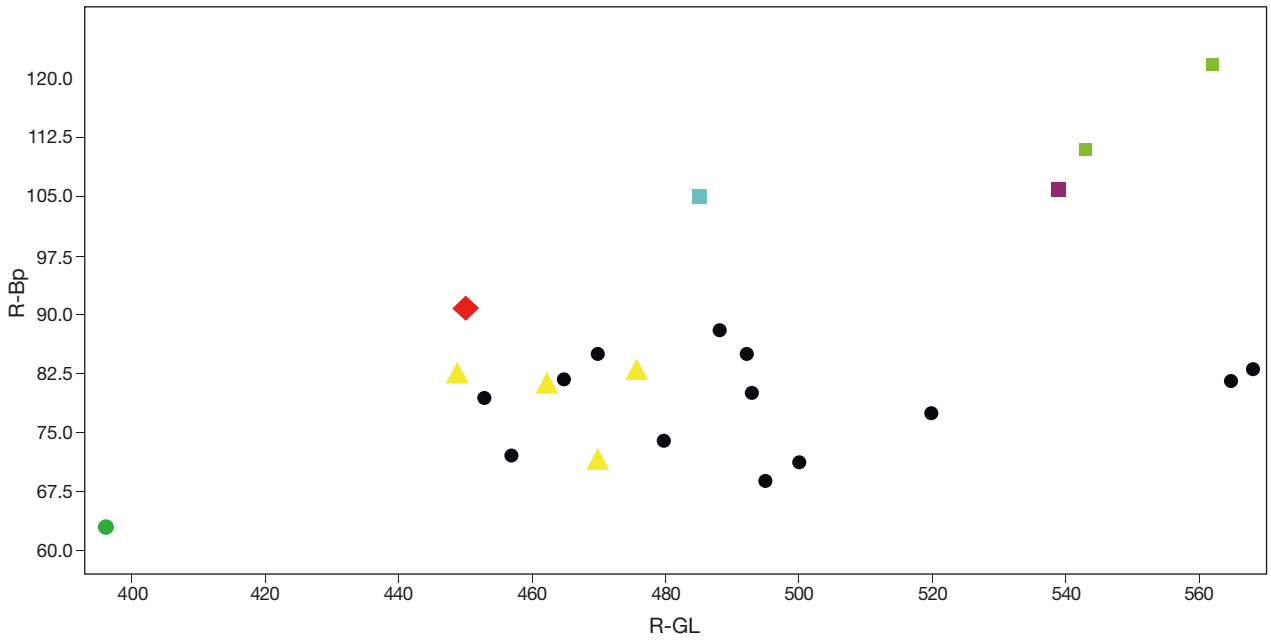


Fig. S5. — Scatter plot of radii proportions of the Late Miocene Eurasian palaeotrages as well as the Nikiti (NKT) sample. Abbreviations: **R-Bp**, breadth of the proximal epiphysis; **R-GL**, greatest length.


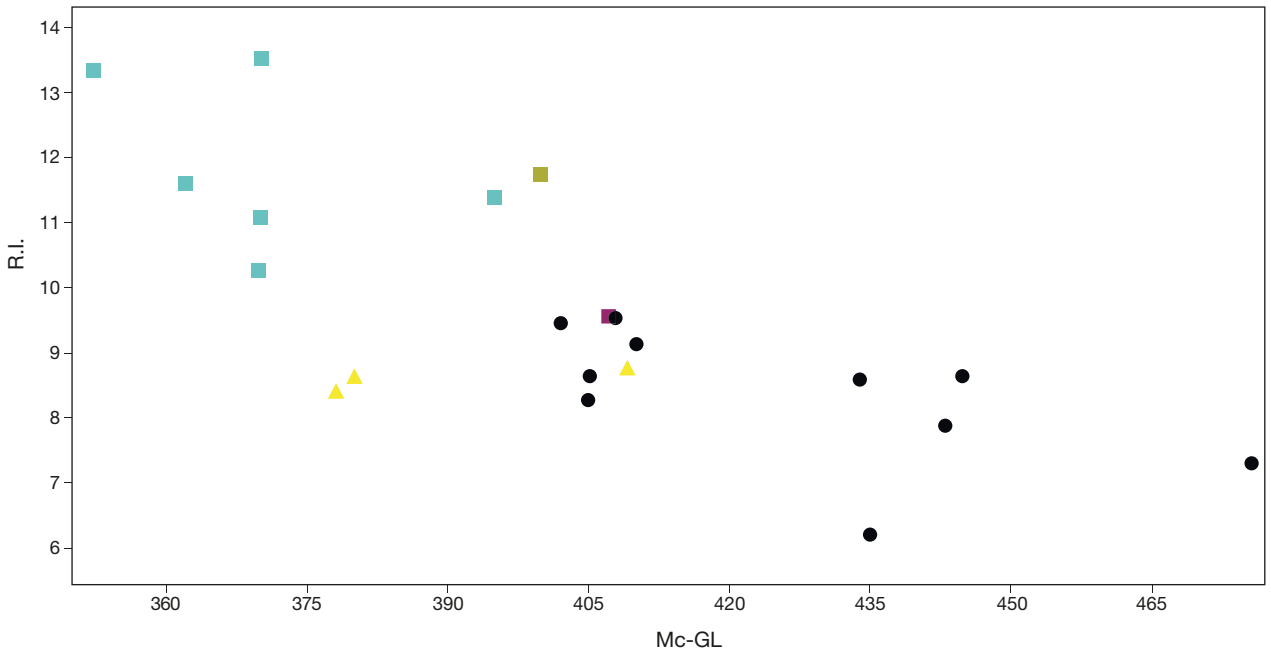


Fig. S6. — Scatter plot of metacarpal proportions of the Late Miocene Eurasian palaeotrages as well as the Nikiti (NKT) sample. Abbreviations: **R.I.**, robusticity index; **Mc-GL**, metacarpal greatest length.

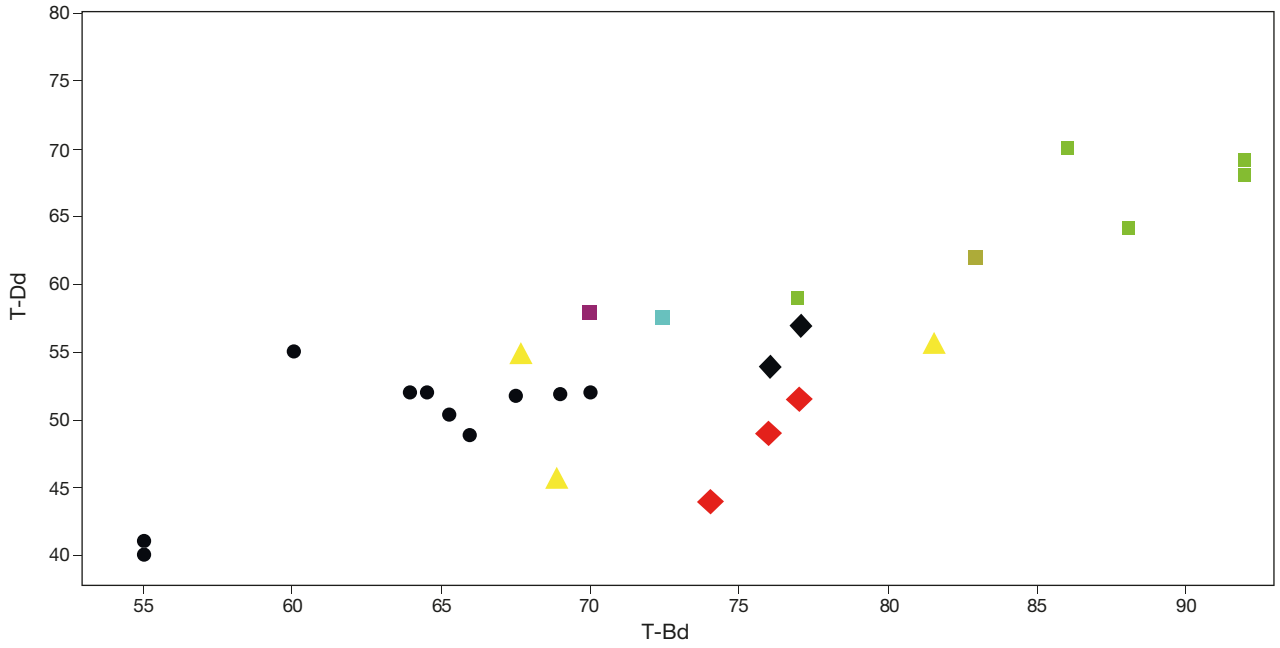


FIG. S7. — Scatter plot of distal tibiae proportions of the Late Miocene Eurasian palaeotrages as well as the Nikiti (NKT) sample. Abbreviations: **T-Dd**, depth of the distal end; **T-Bd**, breadth of the distal end.


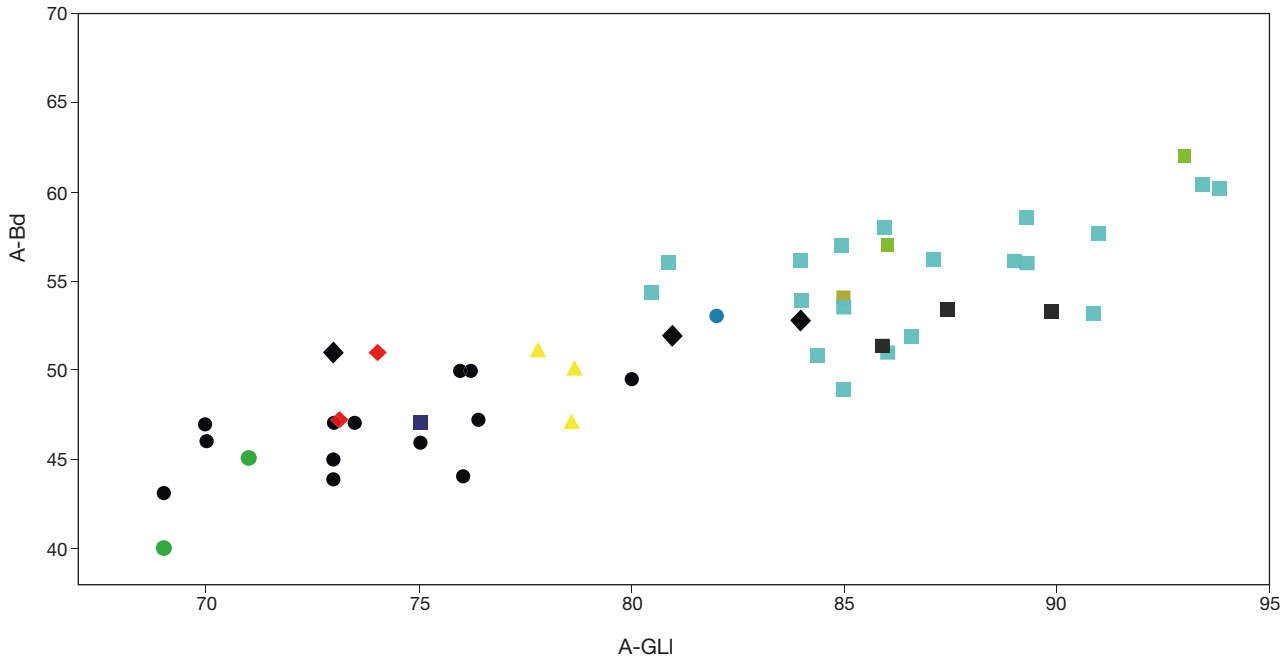


FIG. S8. — Scatter plot of astragali proportions of the Late Miocene Eurasian palaeotrages as well as the Nikiti (NKT) sample. Abbreviations: **A-Bd**, breadth of the distal end; **A-GLI**, greatest lateral length.

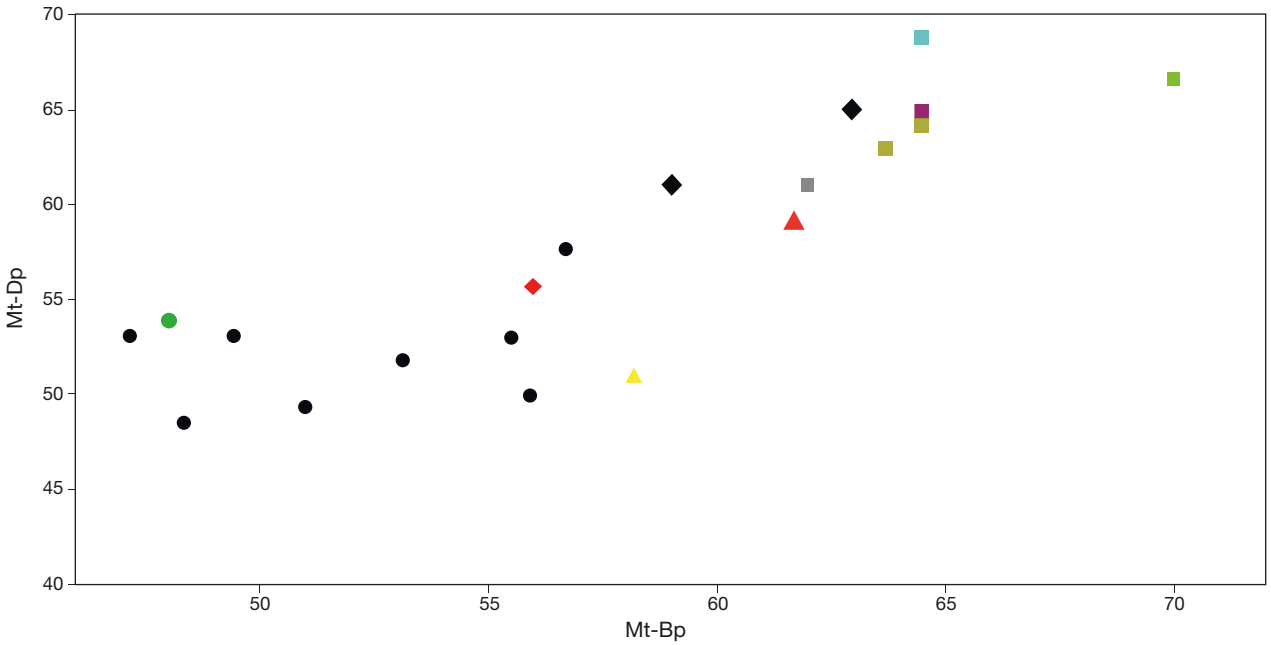


FIG. S9. — Scatter plot of proximal metatarsal proportions of the Late Miocene Eurasian palaeotrages as well as the Nikiti (NKT) and Pentalophos (PNT) samples. Abbreviations: **Mt-Dd**, depth of the proximal end; **Mt-Bd**, breadth of the proximal end.

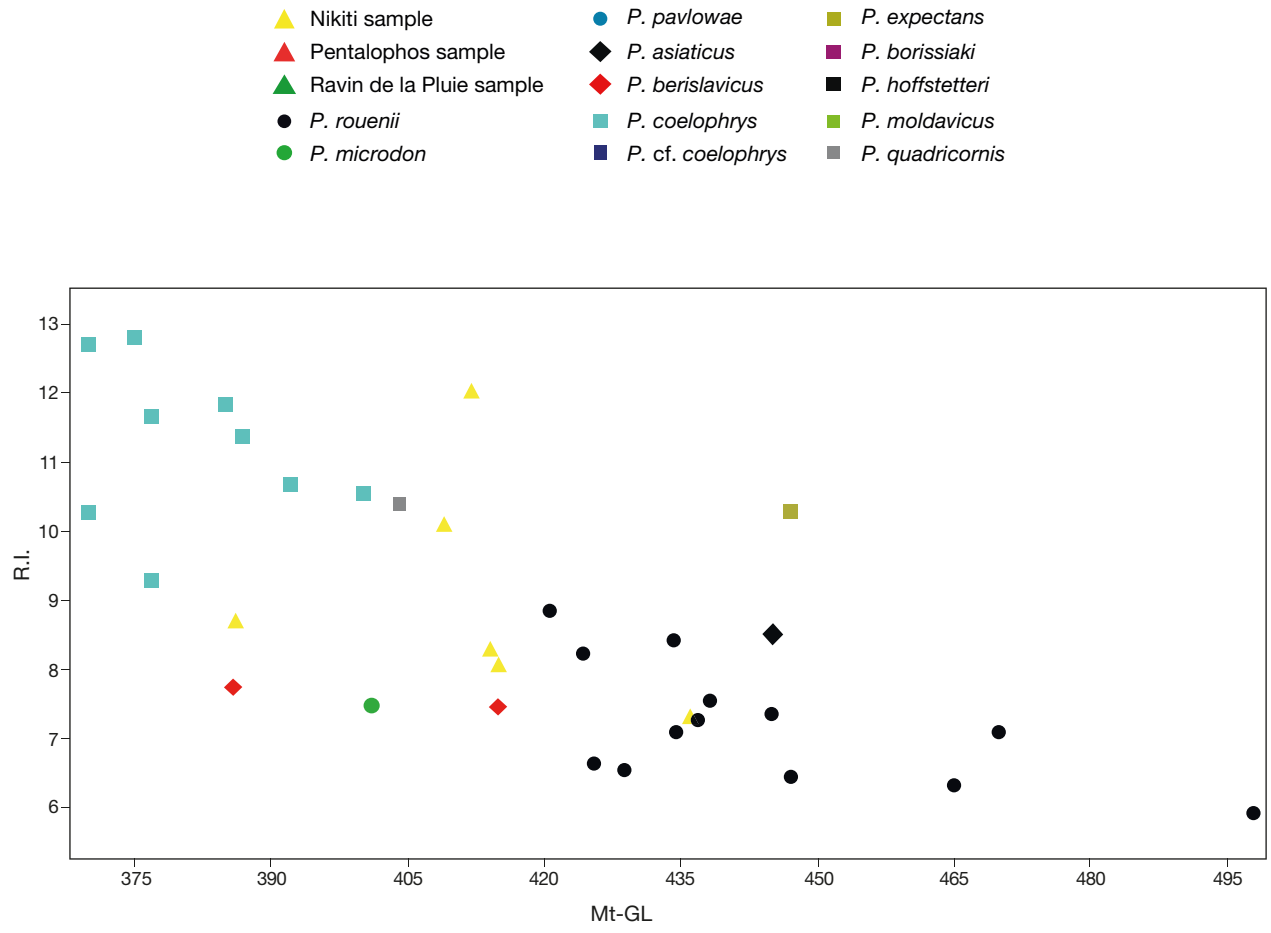


FIG. S10. — Scatter plot of metatarsal proportions of the Late Miocene Eurasian palaeotrages as well as the Nikiti (NKT) sample. Abbreviations: **R.I.**, robusticity index; **Mt-GL**, metatarsal greatest length.

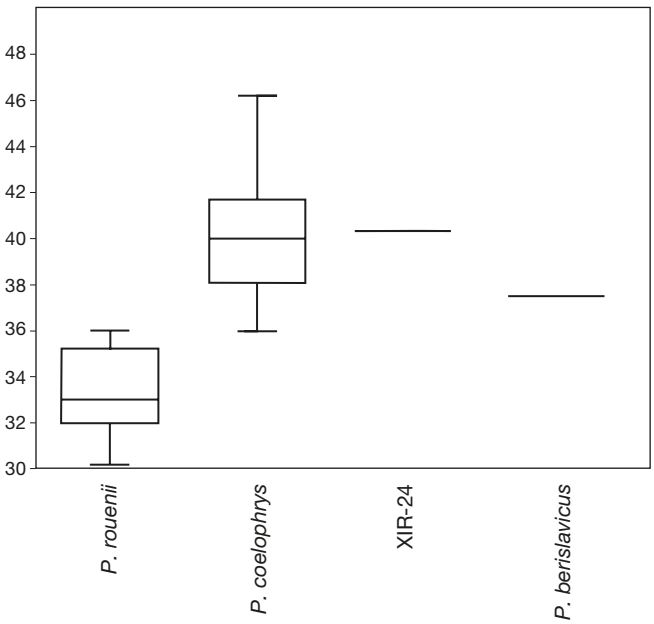


FIG. S11. — Boxplot comparing $M_3$ length among different Late Miocene Eurasian *Palaeotragus* Gaudry, 1861 forms.

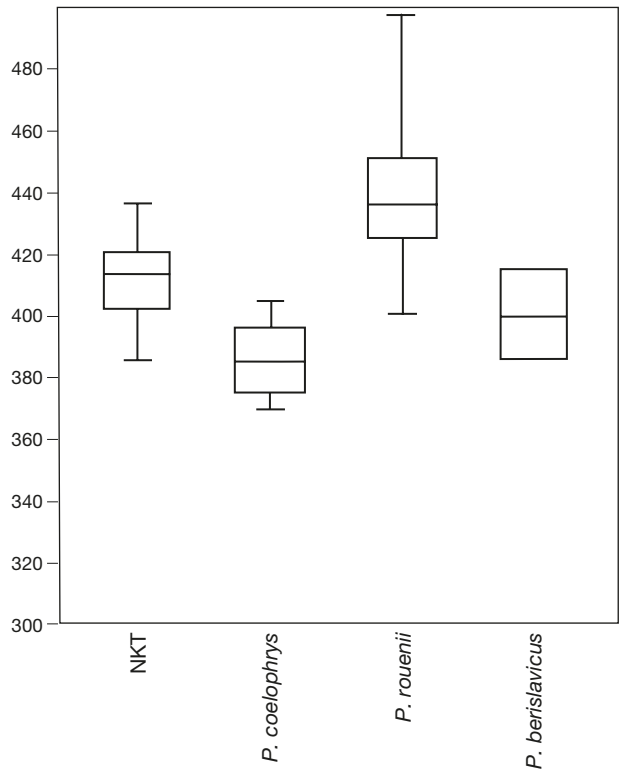


FIG. S12. — Boxplot comparing metatarsal length among different Late Miocene Eurasian *Palaeotragus* Gaudry, 1861 forms.

Appendix 4. — Average measurements of the biometrical variables and the selected premolar features of the Late Miocene Eurasian palaeotrages. Type localities marked in bolt. For character abbreviations see Appendix 1.

| | Site | Lpm | Lp | Lm | Lp/Lm | Lp/Lpm | Lm/Lpm |
|---|---|---|---|---|---|---|---|
| *P. rouenii* | Pikermi | 128.7 | 55.5 | 76.6 | 72.45 | 43.12 | 59.51 |
| | Cimișlia | 130 | 53 | 77.8 | 68.12 | 40.76 | 59.84 |
| | Taraclia | – | – | 78 | – | – | – |
| | Kerassia | 134.95 | 54.85 | 80.9 | 67.79 | 40.64 | 59.94 |
| | Ditiko | 126 | 49 | 78 | 62.82 | 38.88 | 61.90 |
| | Cioburciu | – | – | – | – | – | – |
| | Samos | 128.8 | 50.6 | 78.75 | 64.25 | 39.28 | 61.14 |
| | Todorovo | – | – | – | – | – | – |
| | Kemiklitepe | – | – | – | – | – | – |
| | Novo-Elisabetovka | – | – | – | – | – | – |
| | Strumyani | 122.9 | 47.6 | 75.3 | 63.21 | 38.73 | 61.26 |
| | Hadjidimovo | 129.8 | 51.8 | 78 | 66.41 | 39.90 | 60.09 |
| | Akkasdagli | 129 | 49 | 77 | 63.63 | 37.98 | 59.68 |
| | Thermopigi | 123 | 49.34 | 73.66 | 66.98 | 40.11 | 59.88 |
| | Kryopigi | – | – | 77.6 | – | – | – |
| | Perivolaki | – | 78.6 | – | – | – | – |
| *P. coelophrys* | Maragha | 170 | 65 | 100 | 65 | 38.23 | 58.82 |
| | Samos | – | – | – | – | – | – |
| *P.* cf. *coelophrys* | China | 144 | 56.66 | 87.5 | 64.75 | 39.35 | 60 |
| *P. berislavicus* | Berislav | 152 | 63.6 | 89.7 | 70.90 | 41.84 | 59.01 |
| *P. microdon* | Kansu/Bohlin 1926 | 131.5 | 48.16 | 82.16 | 58.61 | 36.62 | 62.48 |
| | Shansi/1926 | 133 | 50 | 85.5 | 58.47 | 37.59 | 64.28 |
| | China/Bohlin 1926 | – | – | – | – | – | – |
| *P. quadricornis* | Samos | – | – | – | – | – | – |
| *P. asiaticus* | Ortok | – | – | – | – | – | – |
| | Kalmakpai | 141 | – | – | – | – | – |
| | Pavlodar | – | – | – | – | – | – |
| *P. hoffstetteri* | Sinap | – | – | – | – | – | – |
| *P. pavlowae* | Grebeniki | – | – | – | – | – | – |
| | Blagodarnenskaya | – | – | – | – | – | – |
| *P. moldavicus* | Raspopeny | – | – | 98 | – | – | – |
| | Korsakova Assembly | – | – | – | – | – | – |
| *P. borissiaki* | Eldari | 158.75 | 63.5 | 99.4 | 63.88 | 40 | 62.61 |
| *P. expectans* | Sevastopol | 158.35 | 62.5 | 96.25 | 64.93 | 39.46 | 60.78 |
| | Varnitsa | – | – | – | – | – | – |
| *P.* aff. *berislavicus* | NKT | – | – | – | – | – | – |
| *P. coelophrys* | PNT | – | 97 | – | – | – | – |
| *P.* cf. *coelophrys* | RPl | – | – | 89.59 | – | – | – |

Appendix 4. — Continuation.

| | Site | LPM | LP | LM | P/M | P/PM | M/PM |
|---|---|---|---|---|---|---|---|
| *P. rouenii* | Pikermi | 118.2 | 51.9 | 67.33 | 77.07 | 43.90 | 56.9656 |
| | Cimișlia | 114.5 | 50 | 65.4 | 76.45 | 43.66 | 57.11 |
| | Taraclia | 112.5 | 50.25 | 64.75 | 77.60 | 44.67 | 57.56 |
| | Kerassia | – | – | – | – | – | – |
| | Ditiko | 121 | 54 | 73 | 73.97 | 44.62 | 60.33 |
| | Cioburciu | – | – | 64 | – | – | – |
| | Samos | 112.82 | 49.5 | 65.21 | 75.90 | 43.87 | 57.80 |
| | Todorovo | – | – | – | – | – | – |
| | Kemiklitepe | – | – | – | – | – | – |
| | Novo-Elisabetovka | – | – | – | – | – | – |
| | Strumyani | – | – | – | – | – | – |
| | Hadjidimovo | – | – | – | – | – | – |
| | Akkasdagli | 123 | 53 | 72.7 | 72.90 | 43.08 | 59.10 |
| | Thermopigi | – | – | – | – | – | – |
| | Kryopigi | – | – | – | – | – | – |
| | Perivolaki | – | – | – | – | – | – |
| *P. coelophrys* | Maragha | 146 | 66 | 88 | 75 | 45.20 | 60.27 |
| | Samos | – | – | – | – | – | – |
| *P.* cf. *coelophrys* | China | 135.6 | 60 | 81.4 | 73.71 | 44.24 | 60 |
| *P. berislavicus* | Berislav | 138 | 63 | 78.5 | 80.25 | 45.65 | 56.88 |
| *P. microdon* | Kansu/Bohlin 1926 | – | – | – | – | – | – |
| | Shansi/1926 | – | – | – | – | – | – |
| | China/Bohlin 1926 | 123.42 | 54.57 | 71.6 | 76.21 | 44.21 | 58.00 |
| *P. quadricornis* | Samos | 135 | 58.6 | 81.8 | 71.63 | 43.40 | 60.59 |
| *P. asiaticus* | Ortok | 133 | 59 | 78 | 75.64 | 44.36 | 58.64 |
| | Kalmakpai | – | – | – | – | – | – |
| | Pavlodar | – | – | – | – | – | – |
| *P. hoffstetteri* | Sinap | 151.3 | 61.6 | 93.2 | 66.09 | 40.71 | 61.59 |
| *P. pavlowae* | Grebeniki | 127 | 54 | 72 | 75 | 42.51 | 56.69 |
| | Blagodarnenskaya | 127 | 55 | 73 | 75.34 | 43.30 | 57.48 |
| *P. moldavicus* | Raspopeny | – | – | – | – | – | – |
| | Korsakova Assembly | – | – | – | – | – | – |
| *P. borissiaki* | Eldari | – | – | 77 | – | – | – |
| *P. expectans* | Sevastopol | 138 | 62 | 80 | 77.5 | 44.92 | 57.97 |
| | Varnitsa | – | – | – | – | – | – |
| *P.* aff. *berislavicus* | NKT | 143.75 | 63 | 85 | 74.11 | 43.90 | 59.23 |
| *P. coelophrys* | PNT | 138.45 | 59.5 | 82.14 | 72.43 | 42.97 | 59.32 |
| *P.* cf. *coelophrys* | RPI | 149.82 | 65.74 | 89.74 | 74.15 | 44 | 59.33 |

Appendix 4. — Continuation.

| | Site | R-GL | R-Bp | Mc-GL | Mc-Bdia | Mc-R.I. | T-Bd | T-Dd |
|---|---|---|---|---|---|---|---|---|
| *P. rouenii* | Pikermi | 477.4 | 71.5 | 420.15 | 34.8 | 8.28 | 55 | 40.65 |
| | Cimișlia | 492.5 | 83.5 | 425.5 | 37 | 8.69 | 66.6 | 51 |
| | Taraclia | 488 | 86.5 | – | – | – | 70 | 52 |
| | Kerassia | – | – | 445 | 38.4 | 8.62 | 65.3 | 50.4 |
| | Ditiko | – | – | – | – | – | – | – |
| | Cioburciu | – | – | – | – | – | – | – |
| | Samos | 483.75 | 79.58 | 422 | 37.85 | 8.96 | 62.25 | 53.5 |
| | Todorovo | – | – | 402 | 38 | 9.45 | – | – |
| | Kemiklitepe | 453 | 79.25 | 405 | 33.5 | 8.27 | – | – |
| | Novo-Elisabetovka | – | – | – | – | – | – | – |
| | Strumyani | – | – | – | – | – | – | – |
| | Hadjidimovo | – | – | – | – | – | – | – |
| | Akkasdagli | 88.2 | – | 34.4 | – | 67.5 | 51.7 | – |
| | Thermopigi | 568 | 83.21 | 475.79 | 34.5 | 7.25 | – | – |
| | Kryopigi | 500.7 | – | – | – | 7.1 | – | – |
| | Perivolaki | 565 | 84.65 | – | – | – | – | – |
| *P. coelophrys* | Maragha | 485 | 100.5 | 369.8 | 41 | 11.08 | 72.5 | 57.5 |
| | Samos | – | – | – | – | – | – | – |
| *P.* cf. *coelophrys* | China | – | – | – | – | – | – | – |
| *P. berislavicus* | Berislav | 450 | 91 | – | – | – | 75.6 | 48.16 |
| *P. microdon* | Kansu/Bohlin 1926 | – | – | – | – | – | – | – |
| | Shansi/1926 | – | – | – | – | – | – | – |
| | China/Bohlin 1926 | 396 | 63 | 368 | 35 | 9.51 | 55 | – |
| *P. quadricornis* | Samos | – | – | – | – | – | – | – |
| *P. asiaticus* | Ortok | 501 | – | – | – | – | 76.5 | 54.5 |
| | Kalmakpai (Kazhakhstan) | – | – | – | – | – | – | – |
| | Pavlodar | – | – | – | – | – | – | – |
| *P. hoffstetteri* | Sinap | – | – | – | – | – | – | – |
| *P. pavlowae* | Grebeniki | – | – | – | – | – | – | – |
| | Blagodarnenskaya | – | – | – | – | – | – | – |
| *P. moldavicus* | Raspopeny | 552.5 | 114 | – | 45 | – | 87 | 66 |
| | Korsakova Assembly | 107.5 | – | – | – | – | – | – |
| *P. borissiaki* | Eldari | 539 | 106 | 407.5 | 39 | 9.57 | 70 | 58 |
| *P. expectans* | Sevastopol | 108.5 | 400 | 47 | 11.75 | 83 | 62 | – |
| | Varnitsa | – | – | – | – | – | – | – |
| *P.* aff. *berislavicus* | NKT | 464.25 | 81.196 | 389 | 35.79 | 9.2 | 72.67 | 52.09 |
| *P. coelophrys* | PNT | – | – | – | – | – | – | – |
| *P.* cf. *coelophrys* | RPI | – | – | – | – | – | – | – |

Appendix 4. — Continuation.

| | Site | Mt-Bp | Mt-Dp | Mt-Bdia | Mt-Ddia | Mt-GL | Mt-R.I. |
|---|---|---|---|---|---|---|---|
| *P. rouenii* | Pikermi | 48.33 | 48.5 | 32 | 31.5 | 426 | 7.51 |
| | Cimișlia | 55.5 | 53 | 33.5 | 39.5 | 425 | 7.88 |
| | Taraclia | 56.67 | 57.67 | 33.25 | 34 | 436.75 | 7.61 |
| | Kerassia | 55.95 | 49.9 | 36.5 | 41.2 | – | – |
| | Ditiko | – | – | – | – | – | – |
| | Cioburciu | – | – | – | – | – | – |
| | Samos | 53.1 | 51.8 | 31.77 | 35.35 | 445 | 7.37 |
| | Todorovo | – | – | – | – | – | – |
| | Kemiklitepe | – | – | – | – | – | – |
| | Novo-Elisabetovka | 56.67 | 57.67 | 34 | 34 | – | – |
| | Strumyani | – | – | – | – | – | – |
| | Hadjidimovo | – | – | – | – | – | – |
| | Akkasdagli | – | – | – | – | – | – |
| | Thermopigi | 47.14 | 53.1 | 31.37 | 35.26 | 497.79 | 6.13 |
| | Kryopigi | 51 | 49.325 | 31.4 | 37.35 | 467.5 | 6.71 |
| | Perivolaki | 49.45 | 53.05 | 29 | 33.3 | 447 | 6.48 |
| *P. coelophrys* | Maragha | 56.74 | 54.92 | 36.47 | 38.46 | 382.55 | 9.53 |
| | Samos | 54 | – | 35 | – | 377 | 9.28 |
| *P.* cf. *coelophrys* | China | – | – | – | – | – | – |
| *P. berislavicus* | Berislav | 55.96 | 55.62 | 30.5 | 35.67 | 400.5 | 7.61 |
| *P. microdon* | Kansu/ Bohlin 1926 | – | – | – | – | – | – |
| | Shansi/1926 | – | – | – | – | – | – |
| | China/Bohlin 1926 | 48 | 54 | 30 | 38 | 401 | 7.48 |
| *P. quadricornis* | Samos | 62 | 61 | 42 | 42 | 404 | 10.39 |
| *P. asiaticus* | Ortok | – | – | – | – | – | – |
| | Kalmakpai | – | – | – | 453 | – | – |
| | Pavlodar | 63 | 65 | 38 | 45 | 445 | 8.53 |
| | | 59 | 61 | 37 | 42 | | – |
| *P. hofstetteri* | Sinap | – | – | – | – | – | – |
| *P. pavlowae* | Grebeniki | – | – | – | – | – | – |
| | Blagodarnenskaya | – | – | – | – | – | – |
| *P. moldavicus* | Raspopeny | 70 | 66.67 | 46.5 | 44 | – | – |
| | Korsakova Assembly | – | – | – | – | – | – |
| *P. borissiaki* | Eldari | 64.5 | 65 | 44.5 | – | – | – |
| *P.expectans* | Sevastopol | 64.5 | – | 40.5 | 50.5 | – | – |
| | Varnitsa | – | – | 46 | – | 447 | 10.29 |
| *P.* aff. *berislavicus* | NKT | 58.17 | 50.85 | 37.33 | 31.7 | 412 | 9.06 |
| *P. coelophrys* | PNT | 61.68 | 59.16 | 38.93 | 35 | – | – |
| *P.* cf. *coelophrys* | RPI | – | – | – | – | – | – |

Appendix 4. — Continuation.

| | Site | A-GLI | A-Bd | P3 morphology | P4 lingual groove | P4 stylids | P4 shape |
|---|---|---|---|---|---|---|---|
| *P. rouenii* | Pikermi | 71 | 44 | 1 | 0 | 1 | 2 |
| | Cimişlia | 73 | 45 | – | – | – | – |
| | Taraclia | 73 | 45.89 | – | – | – | – |
| | Kerassia | – | – | 1 | – | – | – |
| | Ditiko | – | – | 1 | 1 | 0 | 2 |
| | Cioburciu | – | – | – | – | – | – |
| | Samos | 75 | 47.1 | 1 | 0 | 0 | 2 |
| | Todorovo | – | – | – | – | – | – |
| | Kemiklitepe | – | – | – | – | – | – |
| | Novo-Elisabetovka | 45 | – | – | – | – | – |
| | Strumyani | – | – | – | – | – | – |
| | Hadjidimovo | – | – | – | – | – | – |
| | Akkasdagli | 78.1 | 49.75 | – | 0 | 0 | 2 |
| | Thermopigi | – | – | 0 | 0 | 1 | – |
| | Kryopigi | – | – | – | – | – | – |
| | Perivolaki | – | – | – | – | – | – |
| *P. coelophrys* | Maragha | 86.81 | 55.20 | 0 | 0 | 0 | 0 |
| | Samos | – | – | – | – | – | – |
| *P.* cf. *coelophrys* | China | 75 | 47 | 1 | 0 | 0 | 2 |
| *P. berislavicus* | Berislav | 73.5 | 49 | 1 | 0 | 0 | 1 |
| *P. microdon* | Kansu/Bohlin 1926 | – | – | 0 | 0 | 2 | – |
| | Shansi/1926 | – | – | 0 | 0 | 2 | – |
| | China/Bohlin 1926 | 70 | 39.5 | – | 0 | 0 | 2 |
| *P. quadricornis* | Samos | – | – | 0 | 1 | 0 | 2 |
| *P. asiaticus* | Ortok | 73 | 51 | 1 | 0 | 0 | 2 |
| | Kalmakpai | – | – | – | – | – | – |
| | Pavlodar | 83.5 | 52.5 | – | – | – | – |
| *P. hofstetteri* | Sinap | 87.5 | 51.58 | 0 | 0 | 0 | 1 |
| *P. pavlowae* | Grebeniki | 82 | 53 | – | 1 | 0 | 2 |
| *P. moldavicus* | Raspopeny | 89.5 | 59.5 | 1 | 0 | 0 | 0 |
| | Korsakova Assembly | – | – | – | – | – | – |
| *P. borissiaki* | Eldari | – | 56 | 0 | 0 | 0 | 2 |
| *P. expectans* | Sevastopol | 85 | 54 | 0 | – | – | – |
| | Varnitsa | – | – | 0 | – | – | – |
| *P.* aff. *berislavicus* | NKT | 78.35 | 49.33 | – | 0 | 1 | 2 |
| *P. coelophrys* | PNT | – | – | 0 | 0 | 1 | – |
| *P.* cf. *coelophrys* | RPl | – | – | – | 0 | 0 | 2 |